



UNIVERSITY OF TWENTE.

Faculty of Electrical Engineering,
Mathematics & Computer Science

BLE Localization Using Switched-beam Angle Of Arrival

For Pallet Localization In Warehouses

Thijs de Haan
M.Sc. Thesis
October 17, 2018

Supervisors:

prof. dr. ir. P.J.M. Havinga
dr. ir. W.A.P. van Kleunen

Wireless and Sensor Systems
Faculty of Electrical Engineering,
Mathematics and Computer Science
University of Twente
P.O. Box 217
7500 AE Enschede
The Netherlands

BLE Localization

Using Switched-beam Angle Of Arrival

For Pallet Localization In Warehouses

Thijs de Haan
M.Sc. Thesis – October 17, 2018

Abstract—In the supply chain logistics, a lot of errors can occur that can be overcome by implementing a wireless sensor network (WSN) in the RTI's. This can add a new layer of monitoring to the process. The localization of nodes covers an important part of that. This paper supplies a survey on the architecture, topology and methodology for localizing mobile nodes, specialized on the logistic field. Furthermore, a new circuit board with switched-beam Bluetooth transceivers in eight different directions is evaluated. It can apply the Angle Of Arrival technique to perform localization by comparing a measurement with multiple models. It can reach an accuracy of around 2° in an anechoic chamber, but different altitudes and polarizations from the target severely influence the outcome.

Keywords: Wireless Sensor Networks, Supply Chain, Logistics, Localization, Bluetooth Low Energy, Angle Of Arrival, Switched-beam, Directional Antenna.

CONTENTS

I	Introduction	1	V	Integration	10
II	Logistic Process	2	V-A	Localization protocols	10
II-A	Assets	3	V-B	Localization methods	12
II-A1	Facilities	3	V-C	Localization techniques	12
II-A2	Transporting Network	3	VI	Research scope	13
II-A3	Transport Means	3	VI-A	AOA: added value	13
II-A4	RTIs	3	VI-B	Current Angle Of Arrival Systems	13
II-B	Events	3	VII	Research: switched-beam system test	14
II-B1	Sorting	3	VII-A	Test 1: PCB / Dongle measurements	15
II-B2	Stocking	3	VII-B	Test 2: elaborate 360° rotation measurements	15
II-B3	Check-up	3	VII-C	Test 3: evaluation of theta	16
II-C	Business rules	3	VII-D	Converting measurements to angles	16
III	Positioning in logistics	4	VII-E	Proximity based on RSS	18
III-A	Main focus: tracking and monitoring RTIs	4	VII-F	Calibrating signal power	19
III-B	Properties of localization	4	VII-G	Determining the accuracy of the system	19
III-C	Metrics of localization	5	VII-H	Inaccuracies uncovered	20
III-D	Types of waves and their properties	5	VII-I	Number of antennas	22
III-E	Localization techniques: triangulation	6	VII-J	Indoor experiment	22
III-F	Other localization techniques	7	VII-K	Conclusions	23
IV	Localization composition	8	VIII	Future study	23
IV-A	Localization architecture	8	VIII-A	Improvements	23
IV-B	Localization topology	8	VIII-B	Architecture	24
IV-C	Localization methodology	9	VIII-C	Accurate positioning	24

I. INTRODUCTION

Supply chain logistics involve a huge array of products and services, companies, people, trucks, containers, pallets, warehouses, distribution centres and more. A typical distribution centre or trucking company serves many different customers. Different companies have different procedures, systems and software. Mapping all of that is a challenge in itself – never mind harmonizing it into one, perfectly streamlined process.

Within the field of Wireless Sensor Networks (WSNs), a lot of research has been done concerning mobile nodes, communication and localization. Adding the WSN technology to the logistics will create a new layer of tracking, handling and monitoring the goods which could potentially improve the logistic chain significantly.

This paper is partially to give an overview in how the logistic process basically is arranged, where its challenges lay and how positioning technologies can improve the logistic

process. The main focus is the part of implementing a positioning strategy for the aforementioned purpose. This implies an overview of the architecture, topology and methodology of localization techniques for multiple mobile nodes within a static, arranged environment.

This overview then comes to the proposal of a research within the subject. After the analysis of different techniques and systems, a strategy is chosen and research questions have been formed to find out how the system can best be integrated to use in practice.

The paper concludes with the report of a research of a possible device that could be used for angulation to localize Bluetooth nodes within a warehouse. This device was tested in an anechoic chamber, from where models were created on how signals from different angles are being received and how accurate this angle can be derived.

Similar studies

There is a lot of research performed on WSNs and localization. This type of scenario which is very dynamic, uses a lot of nodes on batteries and many gateways, is specified more particular as Dynamic Wireless Sensor Networks (DWSN).

The specific case for localization within logistics was introduced by Patwari et al. in 2005 [1]. It mentions J. Kumagai and S. Cherry who described what probably is the first large scale application of RFID technology within logistics. Readers at the warehouse loading docks of a port scan each pallet and case of goods automatically, reducing labor costs, theft, and errors [2].

The case is further elaborated on by Evers et al. in 2005 [3]. In 2007, Evers et al. presented Sensorscheme: a platform for realizing a specific scenario within the same topic [4]. The paper focusses on the proceedings of an individual node and involved business rules, not so much on the localization part. Fogel et al. elaborated on the localization of pallets in warehouses using the combination of radio waves and ultrasound chirping [5]. They did a research with the assumption of Line of Sight (LOS), which is not very realistic: the lack of LOS is almost inevitable and will have a big impact on the accuracy of the positioning. Spieker and Röhrig analyse the applications of a special sensor network (nanoLOC System) for operations within the warehouse management [6], 2008. They achieved less than half a meter accuracy on an approximately 9x3 meter rack using four beacons and measuring the Received Signal Strength with LOS. Measurements without LOS lead to an error of more than a meter.

Bijwaard et al. went to the case of cold chain logistics and presented a WSN with SmartPoints: nodes that collect data, connect to an ambient network and via internet to a BackOffice application [7]. This case is particularly interesting because of its focus on the communication issues that occur.

The main topic where this paper distinguishes itself from earlier researches about the same topic, is the focus on finding a localization strategy that is applicable in warehouses of various dimensions that is robust to no LOS.

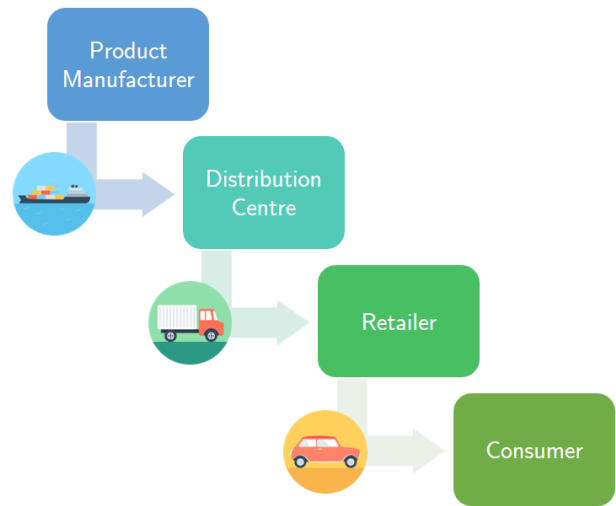


Figure 2.1: Logistic chain from factory to end consumer

II. LOGISTIC PROCESS

The logistic process is all about transporting goods from a source to a destination. Goods are wrapped up and often merged together in packages, transported among maybe thousand other packages at the time. Using multiple transportation vehicles, they are brought to several places where they have to be sorted again to be transported to the next place before they reach their destination. To give an indication, a regular product follows the stages as displayed in figure 2.1. Based on the destination, a transport plan is constructed. The first stage is a shipment over a long distance. Goods are transported towards the harbour, sorted, loaded onto the ship, unloaded at the next harbour, sorted again and transported to the distribution centre.

Once at the distribution centre, it needs to be sorted again and perhaps the quality needs to be checked. The instructions for each package or load is shared in advance via internet and paperwork. Tens or hundreds of employees form a part of the system that performs the sorting and checking. Packages furthermore have to be stocked among hundreds or thousands of other goods inside a warehouse, for a definite or indefinite amount of time before they get processed again for departure. After one or maybe more distribution centres and several cases of sorting, stocking and check-ups, the next step of the product is to get sent to a consumer via a courier company or via a local shop like a retailer. The sorting centre or retailer has its own warehouse where the sorting, stocking and quality check are performed again.

There can also be multiple parties involved in the logistic process. To name just a few: a company that produces a product, a company that facilitates gear like a trailer, pallets or containers, one or more companies that take care of the transportation of these gears and those of other parties, a warehouse that stores and distributes the goods, a store and of course a customer. It is ought to be clear that the scale and complexity of rural logistic processes is huge and challenging. Even if the chances of any mistake occurring are small, the impact is tremendous. Goods might get lost, damaged, brought to the wrong place or be delayed, and the source of any

disturbances might not even be able to be traced. If anything in the chain goes wrong, all the later stages of the chain are affected by it. If a part of a load is missing on a truck, the truck will not be fully packed and another truck will have to collect the missing packages afterwards, severely decreasing the efficiency. Solving this complex issue would save a lot of time, money and waste.

A. Assets

For the transportation, holding, protection and securing of the product, several assets are used. The following need to be distinguished.

1) *Facilities*: static environments in which the sorting or stocking takes place. In most cases this is a building, but it can be a parking lot as well. A warehouse, the typical place where the localization becomes most relevant, is an environment that brings several challenges. The buildings can be very large, so it might require a lot of gateways and beacons to cover the whole area and these must cooperate with each other in one system. The roof can be very high, which will become a challenge for localization when the beacons are so high from the ground. The nodes that have to be positioned inside can become large in numbers, condensed and stocked on top of each other.

2) *Transporting Network*: the physical network that provides the connection between facilities, like for example roads, rails, waterways, the airspace, pipelines or even wires. It also includes internal transportation provision within a facility – the so called intralogistics – where the conveyor-belt is a typical addition to the mentioned examples.

The *modality* is a term to define the mode of transport: the use of a transporting network including possibly a transport mean. If multiple modalities are used to transport a product, we speak about multimodality or intermodality.

3) *Transport Means*: the vehicles that are used for transporting the goods among different distribution centres or facilities. These include trucks, tractors, ships, trains and airplanes.

It also includes *materials handling*: the management of transporting goods within a facility. This includes forklifts, warehouse trucks (like narrow-aisle trucks, order picking trucks, stackers or pallet transfer trucks), Automated Guided Vehicles (AGV's) and a crane [8].

Finally, non-vehicle or manual movement (transportation by hand or using a manual pallet truck) is also considered a transport mean.

4) *RTIs*: a Returnable Transport Item is used to store goods and being able to transport, and be returned and reused an indefinite amount of times. There are roughly three types of RTIs to be distinguished: transport equipment, load carriers and secondary packaging.

“Transport Equipment is defined as a piece of high-value equipment used to hold, protect or secure cargo for transportation purposes.” [9] One can think of trailers, wagons or intermodal containers. Load carriers are smaller and cheaper like pallets, roll containers, dolly's, garment racks et cetera. Secondary packaging like totes, buckets and plastic crates are smaller and suitable to carry by hand.

B. Events

As mentioned before, the goods might be sorted, stocked or checked for their conditions at a facility like the distribution centre.

1) *Sorting: identification and transportation to a destination within the warehouse*. For decades, Optical Barcode Systems (OBS) are used to identify packages. The barcode needs to be scanned by an employee which monitors and tracks the package. This is time-consuming, error-prone and only allows discrete-time tracking [3]. Furthermore, RFID-tags are sometimes used instead of the barcode. This has some advantages but the essence, identification, is the same. It is possible that barcodes or RFID-tags get damaged or mistaken when an expired one is still present at the RTI.

Information about the RTI is gathered in the database of the Central System (CS). Via internet, this information is retrieved from a back-end server. The RTI specific instructions are translated by the CS into order associations which are synchronized with the RTI its node and transmitted to the employee.

Once an RTI is identified and the destination is known, it is transported to for example a sorting spot: a square drawn on the ground. There might not always be space enough in the sorting spot and this process is vulnerable to human errors. From a sorting spot, RTIs can be loaded onto a truck. Another destination can be the local stock.

2) *Stocking: keeping the package for a short or longer period in the storage of a warehouse*. In big warehouses they use dozens or hundreds of tall racks for this, which creates a organizational challenge. A computer is often used to take care of this: it assigns a spot and registers the RTI so it cannot get lost or be forgotten. A narrow-aisle truck is used to guide the RTI to the right spot. In some warehouses, this transportation is partially or fully automated in order to prevent any mistakes.

3) *Check-up: quality of the load and satisfaction of the stocking conditions*. Most packages do not have more requirements than to be kept dry and at usual temperatures. Other supplies might be more demanding. For example the temperature in cold chain logistics must be treated very delicate. Other packages contain very fragile goods so heavy bumps are prohibited. Another possible constraint is gasses in the air: some goods like bananas must not be stored close to goods that contain coffee beans that emit ethylene gas, influencing the bananas ripening process. Some gallons of liquid corrosive (acid) material cannot be stored within 6 meter from a base and a flammable material cannot be stored within 6 meter from an oxidizer. All these constraints that are bound to an individual RTI need to be met, which is a major challenge. Violation of these stocking conditions and damaging of the load needs to be traced, corrected, logged and passed on to the back-end server.

C. Business rules

Figure 2.2 shows a simplified diagram of the process for any RTI that is being transferred. There is a distinguish between four stages and each stage contains its own *business rules* (BRs). All the BRs that contain an asterisk, have potential to be

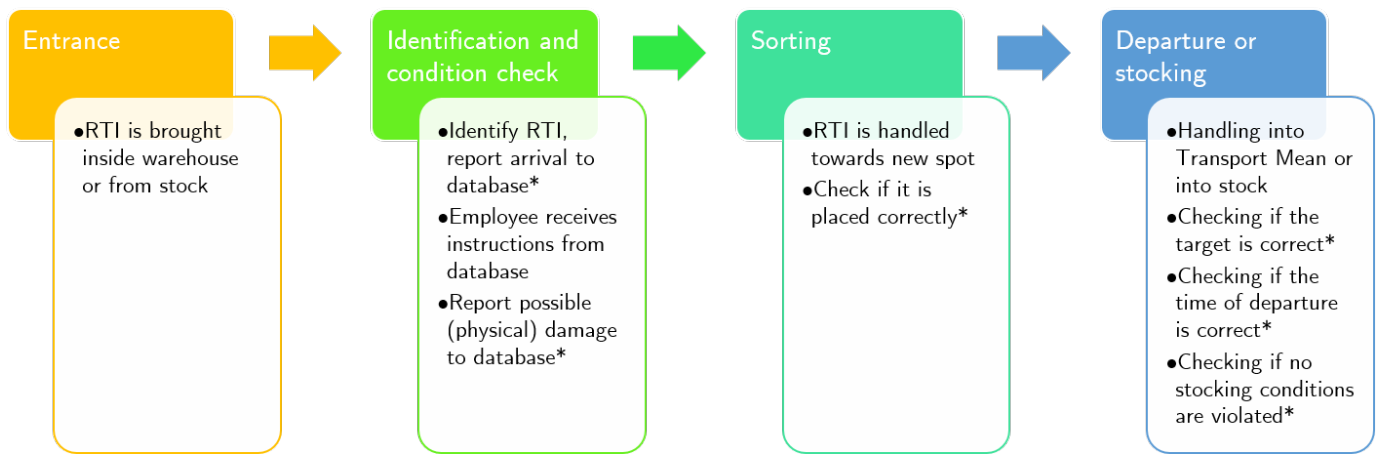


Figure 2.2: Transportation process and business rules within a warehouse

partially or fully covered by a system with wireless connected nodes integrated in the RTIs.

In case of damaged goods, an employee is still required to perform a check. However, an integrated temperature sensor and accelerometer in the RTI can recover more information about possible damages than is visible at first glance, and it can keep log of relevant events. These logs are shared with the Central System (CS) and passed on to the back-end server. Also the moments of arrival and departure are relevant for the CS to derive and passed on to the back-end server.

Considering all the check-ups, they are at risk to be omitted by the employee. An autonomous node that is integrated in the concerning RTI and is able to localize itself and interact with a CS, can easily cover this part of the BRs and thus give useful support. The next chapter elaborates on how this system might look like.

III. POSITIONING IN LOGISTICS

The rest of this paper will focus on positioning within the logistics only. The distribution of data and the data logging are omitted. The stocking conditions check however, will be discussed regularly because it is closely related to the property of positioning.

A. Main focus: tracking and monitoring RTIs

For a better control on the logistic process, it is interesting to follow the path of a product more accurate than is accomplished nowadays. One can for example trace the transporting equipment that transports an intermodal container, trace the container that contains pallets, trace the pallet that carries boxes, trace the box that carries goods and trace the goods themselves. Ideally, all the goods can be traced. In practice, this is a bit redundant: multiple goods with the same destination are often bundled within an RTI for their whole journey. Workers at a distribution centre think in terms of those RTIs, not what they contain. It is more likely that an RTI gets lost in the process than that a product separates from an RTI, and it is more lucrative to solve the loss of an RTI than possible lost products. It makes therefore most sense to focus on the RTI in the form of load carriers like a pallet

or roll container. Furthermore, it would be fruitful to monitor behaviour and circumstances of each RTI: measure clashes and temperature changes, log it and send out a warning if necessary. Nowadays RTIs are tagged with a barcode or RFID-chip, which requires a user to scan and verify its location. Enabling the RTI to be localized from distance or localize itself using radio communication, creates the opportunity for real-time tracking and to add a new layer of monitoring the RTIs.

B. Properties of localization

Concerning positioning, there are several properties to take into account. For different positioning applications, the properties basically tell what the method is capable of – regardless of how good it performs in it.

Within a warehouse, a **coverage** of all three dimensions are relevant: RTIs can be stored high up in a rack [10]. Within a truck, it might be useful to know which RTIs are in the back or near the entrance.

The **physical** location of a mobile target is expressed in the form of coordinates, like from GPS. The **absolute** location is the three dimensional position of the node within a shared reference grid for all located targets [11, 12].

The reception of a signal gives information of the **proximity** between two devices, like that a node is located near beacons or among other nodes. This is actually a positioning technique (mentioned in section III-F). By estimating this distance, the **relative** position can be derived between the nodes or beacons.

Related to this is **symbolic** localization: a target is located in a room, on a sorting spot, on a rack or near the entrance of a building. A node can derive that it is on the right sorting spot if it knows that its surrounding nodes have the same destination, or derive that it is at the wrong place if its destination differs from that of surrounding nodes. Furthermore it might be able to approximate its position based on the **number of hops** to a gateway or node of interest.

The **view direction** is difficult to obtain using a node with an omnidirectional antenna. There are however possibilities to retrieve it. Navigation systems for example derive it from the

moving direction. For a pallet, it would be useful to retrieve the view direction if the antenna is located at the side of the pallet: that would determine on which side of where the device is positioned, the corresponding load is located. This does not account for a pallet with the antenna in the center.

It is useful for an RTI to be able to detect **movement**. When static, both the Central System (CS) and the RTI know its position. When the RTI detects movement, it knows that it is being handled and that its position will be changed. This information is also relevant to the central computer so this can be communicated. While being transported, it is optional to track the movement.

C. Metrics of localization

Different techniques have their up and downsides. The performance of positioning systems are expressed in terms of metrics. The choice of a technique that is suitable for a certain application is made by making a trade-off between performance metrics described in this section.

The **responsiveness** means how often a nodes position is updated per amount of time [10]. It makes sense that if a node stays unmoved within a static environment, it is sufficient to determine its absolute position only once. However when it is moved, the position becomes uncertain and the positioning frequency should go up in order to keep track of its position. Considering its relative position, it is often based on dynamic surroundings like other nodes: they can change over time. When a node needs to keep track of these changes – for example when goods of other RTIs can cause harm to the goods in its own RTI – it should regularly re-determine its relative position. There can also be a scenario where the composition of RTIs does not change, like when they are being shipped in a container. For a node that takes note of this, it is sufficient to determine its relative position and surroundings only in the early stages when it is loaded.

Some positioning methods are more **accurate** than others. Usually, the accuracy is expressed as the average Euclidean distance between real and estimated location [10, 11]. **Precision** can be defined as “the success probability of a position estimation with respect to the predefined accuracy” [13–15]. It makes sense that the error should be less than 80 centimeter for the case of ordinary 0.8 by 1.2 meter pallets that need to be positioned at racks with 1.5 meter high floors. Of course the required accuracy can vary. One could afford a bigger error when a target is traced during transportation. The exact position is obviously changing and it is now relevant to know what its direction is. To find that out, the position should now be calculated more regularly - say once every four seconds. With an accuracy of less than five meters, it is still possible to derive the movement of the pallet over the big and long trajectories within a warehouse.

The **complexity** of the localization algorithm should be feasible: the computing power and battery supply of a node might be limited [10, 11]. The Central System (CS) should be capable to handle more complexity. Hardware, software, and deployment can form an issue [15].

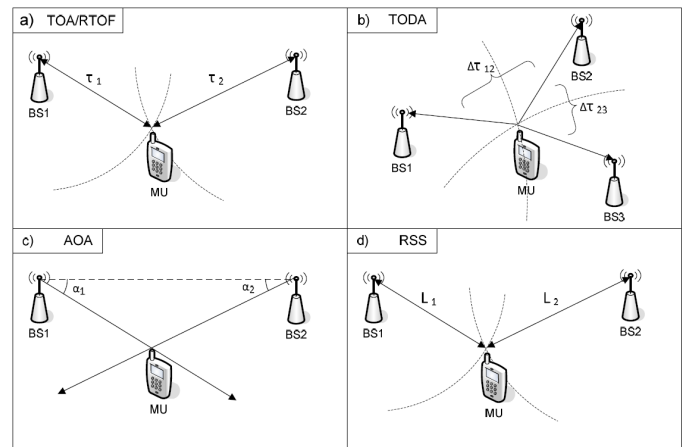


Figure 3.3: Four measuring methods for triangulation, obtained from [16]

The performance might be influenced by changing environments: the localization of an RTI in an empty warehouse will be far more accurate than when it is surrounded by goods. The system must be able to handle these disturbances, what is called **robustness** or **adaptiveness** [10, 11, 15].

The system must also be **scalable** [10, 11, 15]. It might be affordable to place less beacons in a warehouse and cover a bigger area per beacon, but the accuracy will then decrease and the system will be less capable of handling a large amount of nodes.

The system must be affordable. The **cost** of the installation, maintenance and power consumption of the nodes, beacons and CS can become an issue [10–12, 15]. At least, the cost must not exceed the benefits.

An elaborate overview of the up and downsides of different positioning methods in terms of metrics is given in [15].

D. Types of waves and their properties

Waves occur in a lot of forms and circumstances, with various properties. Often used in WSNs are acoustic, radio and optic waves.

All three of those types have the ability to provide communication and localization, but there are some up and downsides. Acoustic waves use a relatively low frequencies. The audible frequencies and low ultrasound frequencies are often used because they propagate best in air. Higher ultrasound frequencies are often used underwater. Generally, higher frequencies have bigger attenuation. A low frequency implies a smaller bandwidth and, according to the Nyquist formula, it can carry less information. In addition, acoustic waves are way slower so they bring are even more challenges like a higher chance of collisions between messages.

Optic waves use a very high frequency, which can carry a lot of information, but for a price: waves are easily absorbed by materials and do not move around corners (diffraction, which occurs when an obstacle or hole is smaller than the wavelength). The result is shadowing: large regions where the

signal is lost. To use optical communication, Line of Sight (LoS) or at least high-quality reflections are required.

The frequencies of radio waves are precisely in between these spectra. Depending on the frequency, the properties of diffraction and penetration of objects can be achieved and a high data rate can be facilitated. Especially the UHF band, the spectrum between 300 MHz and 3 GHz, is widely used for any communication network.

Propagation and fading

One important property of a wave for localization is the propagation. If a wave propagates isotropic, the power of the signal decreases exponentially with the distance. However, most antennas are not perfectly isotropic and signals might be absorbed by obstacles, resulting in large scale fading. Furthermore, the signal will be diffracted, reflected and scattered, leading to multipaths and self-interference [17]. All these effects of small scale fading will influence the strength of a signal at a certain point where it might be received. Small scale fading depends on the frequency: it is possible that some specific channels are in a frequency dip. A simple but widely used solution is to use more frequencies, called spread spectrum. This will give a better accuracy in localization.

E. Localization techniques: triangulation

There are three important properties of waves that are used to derive the location of the source: its direction, the attenuation and the duration of its propagation. Respectively, the **Angle of Arrival (AOA)**, the **Received Signal Strength (RSS)** and the **Time of Flight (TOF)** can be measured. The process to determine the location from these properties is called triangulation. It consists of two methods: **angulation** where the AOA is used to determine an angle and **lateration** where RSS or TOF are used to determine a distance from source to measurement spot [10, 11, 15]. If lateration is used, the method should be called trilateration instead of triangulation. This term is however not very familiar.

The angulation method (sometimes called DOA from Direction Of Arrival) requires a measurement point that has directional antennas or an array of antennas [11, 15]. Based on the strength of reception on different pre-defined angles, the position of the source of a signal can be derived relative to the measurement spot. The distance is unknown, so at least two measurements are required to approximate the exact position.

This method is often used for 2-D positioning, because two measuring devices only derive the angle in two dimensions. It is possible to use a third device that oriented differently, in order to obtain the angle in the third dimension .

Note that the reliability of this method might be influenced by small scale fading and the accuracy degrades as the target is further away from the measuring unit [11, 15]

The lateration method is used to calculate the distance from source to measurement spot. It can be **RSS-based** (or Signal Attenuation-Based) or **TOF-based**.

The RSS-based method implies deriving the distance between the mobile target and the measurement unit using the signal's attenuation. The RSS-value is compared with a theoretical model in order to determine the corresponding range [11, 15, 18]. The attenuation is very vulnerable to large-scale fading and is also non-linear. Furthermore, measured RSS-values are influenced by multipath fading [17]. For example, a dipole antenna does not emit the same strength to every direction and waves can be reflected or absorbed by the environment. Besides a theoretical model, empirical models can be used based on first collect features (fingerprints) of a scene. This is known as the **Fingerprinting based** or **Scene Analysis** method [11, 15].

The TOF-based method implies deriving the distance by multiplying the TOF with the radio signal velocity. TOF can be used for trilateration or multilateration: the use of three or more reference points. With only one beacon that derives its distance to a target, only a circle (or sphere in 3-D) on which the target might be is known. In order to approximate the exact location, at least three distances must be used for reference [11]. It is also possible to achieve this with a combination of angulation and lateration: for example when one measuring unit derives both the direction of the signal and the distance to the source. However, given the possible indoor lack of Line of Sight and multipath propagation, it is advisable to gain multiple references and use a weighted least-squares algorithm in order to obtain a better accuracy.

The TOF can be derived from the **Time of Arrival (TOA)** when the time of emission is known. The only way to achieve this is to synchronize the clocks between the node and beacon very precisely: every ns error creates 30 cm positioning error. There are also methods that do not require clock synchronization with the target.

Because sound is so much slower, its TOF is easy to compute when it is combined with radio communication. An application is can be found at the Cricket localization-support system that makes use of ultrasound transmitters [12, 19]. The sound wave is only used for distance estimation, not for data transmission.

One way to measure distance with radio without clock synchronization, is by measuring **Round-trip Time of Flight (RTOF)**. The technique is also called Two Way Ranging (TWR). This means that measuring unit sends a signal to the target, waits for response and measures the time in between or the Round Trip Time (RTT). Subtracting the processing time at the other device results in twice the TOF. This technique requires an extra transmission per measuring device. Another difficulty is the error caused by clock crystal drift between the nodes. A more advanced version of this is Symmetric Double Sided Two-Way Ranging (SDS-TWR). This method uses three messages to estimate the distance and reduce the error from the clock drift [20]. Usually, these three messages form one computation and from multiple computations, an average is taken. For 3-D positioning this needs to be performed with at least three reference points.

Another way to determine the TOF without synchronizing the clock between transmitter and receiver is by measuring the **Time Difference of Arrival (TDOA)**. This requires at least

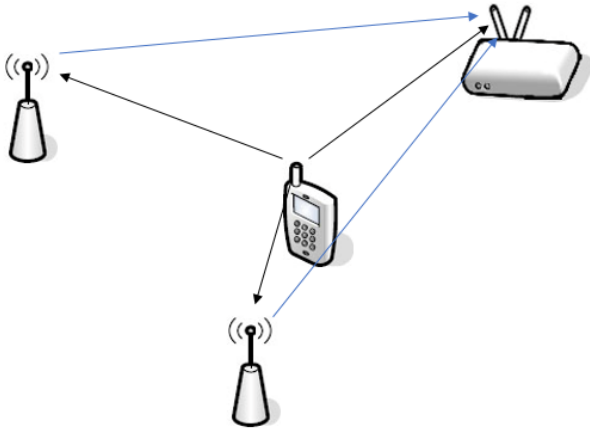


Figure 3.4: TDOA-FC: TDOA without time synchronization

three pairs of reference points with a known location where the TOA is measured. From the differences, the relative position of the mobile target with respect to the reference points is calculated [10, 11, 15]. Note that the TDOA techniques does not require time synchronization with the mobile target, but it does for among the receivers. This is a bit complex, especially when performed over a huge area containing tens or hundreds of receivers.

Because both RTOA and TDOA suffer from inaccuracies caused by the clock drift, usually multiple measurements are performed to take an average. A better accuracy therefore requires more time, energy and use of the ether from the components.

There is also another possibility for TDOA to position a target, using the RTOA principle to bypass the requirement of time synchronization. Imagine beacons, placed like a hexagonal grid, with a gateway in the middle of each hexagon. Two neighbouring beacons form a triangle with a gateway nearby. This setup is illustrated in figure 3.4. Just like with RTOA, the beacons retransmit a message, only this time it is forwarded to the gateway. Because the distance to the beacons is known, the TDOA can be derived for all three of the receivers and the distance to the mobile node can be calculated. The technique will for now be called **Time Difference of Arrival using Forwarded Components** (TDOA-FC). The gateway should be able to maintain a connection with six beacons (better called forwarders) and mobile nodes at once. The grid does not necessarily have to be hexagonal: with a square grid, the gateway only needs to connect with four forwarders. Each forwarder should have its own channel and should not forward messages from other forwarders, leading to endless repetition. A simple solution for this is when they identify themselves in every packet they (re)transmit.

The big problem with this new introduced technique is that it is more difficult than to apply time synchronization and use TDOA. The forwarder will again have the problem of clock drift. The way to overcome this would be to design a protocol where the forwarders and the gateway synchronize with each other at every measurement. The advantage is that this method might exempt the mobile node from some transmissions, but

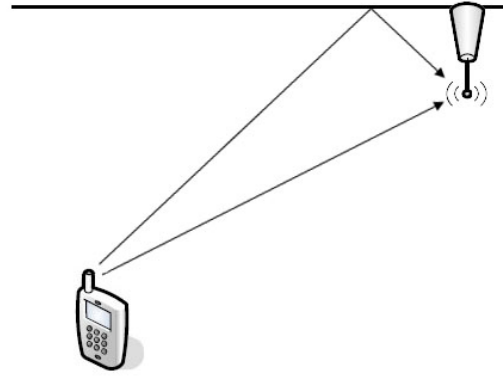


Figure 3.5: TDOA-MC: TDOA and AOA with one reflection

it needs to be developed yet.

The authors of [21] found a way to measure the distance to a target with only one antenna and no need for time synchronization, measuring the multipath components. This is called **Time Difference of Arrival between Multipath Components** (TDOA-MC). This can be translated into figure 3.5. If the (perfectly flat) ceiling would provide a good reflection, both the distance and angle can be measured based on only one signal. Of course the reflection will interfere with the original signal, leading to a probably even bigger challenge.

Another option is the use of array antennas. If two antennas are very close to each other (less than half the wavelength), they experience a tiny delay if the signal arrives with an angle. From this delay, the AOA can be derived. If three of these antennas are placed in a triangle, a measuring device is created that can derive a 3-D angle. Elaborate systems even use a big grid containing small antennas, so the AOA is measured on a whole surface. All these measurements can be combined to perform triangulation and trace the source its position with only one device. This is for example used in modern radar equipment.

F. Other localization techniques

Besides triangulation, there are some other techniques worth mentioning. One is already mentioned briefly in section III-B: **Proximity Detection** (PD) or Connectivity Based Positioning. When there is a grid of antennas, the mobile target is considered to be collocated with the antenna that receives the strongest signal from the target. This method is easy to implement and is for example used to detect mobile phones in cellular networks, called Cell Identification (Cell-ID) or Cell Of Origin (COO) [10, 11, 15, 17]. The barcode system that is being used extensively, is also considered as a PD localization technique. This system is sometimes replaced by RFID, which has no optical requirements and can be scanned from a longer distance. An employee can sometimes scan multiple tags at once and gates can be used to scan any tag that comes through.

Positioning is limited by responsiveness: there are gaps between two updates in which the position is uncertain, but

can be estimated based on the last known direction and speed. This method is called **Dead Reckoning (DR)** and the accuracy can be improved within the node itself, using sensed data of movement [10, 15, 22–24]. The accuracy of this method decreases with time because new positions are estimated entirely based on earlier ones.

A more advanced version that combines DR with other data is **Map Matching (MM)**. This method is about using sensed data of movement (like performed in [24]) and collecting fingerprints as mentioned in section III-E (Scene Analysis, SA), or more explicitly: detecting beacons like a gateway or tag. The authors of [17] for example used ZigBee nodes as beacons. Using the theory of pattern recognition [25], all this data is evaluated using a pre-composed map in order to find a spot that matches the data as accurate as possible. Another example: the sensing of a bump can be accurately matched to a doorstep on the map. “MM techniques include topological analyses, pattern recognition, or advanced techniques such as hierarchical fuzzy inference algorithms.” [10] The method can be very complex.

Each technique has its advantages and disadvantages. To use the benefit of multiple techniques, combinations or **hybrid techniques** have much potential. An overview of all the techniques and possible hybrids is given in [15].

IV. LOCALIZATION COMPOSITION

As mentioned in section III, localization can be achieved using the direction (angle), signal strength or time of flight of a signal. This chapter looks into the subject of localization from the perspective of architecture, topology and methodology.

A. Localization architecture

Looking at the architecture, we distinguish between dynamic and static assets. The facilities and transporting network are typically static, while RTI’s and transport means are typically dynamic. Nodes can be fixed, like beacons that are constructed at fixed locations in a warehouse. If nodes are mobile but their location is known, they function as anchor: other nodes can determine their position based on the anchor nodes [10, 15, 26].

It is also possible that the transport mean, for example a truck, is equipped with a node that has GPS information. In this case the node functions also as an anchor node. Of course, the accuracy of GPS is limited so using the truck its node for reference is a totally different approach than the indoor beacon localization. However, the infrastructure is basically the same.

B. Localization topology

This section looks at different setups where different ways of localization can be realised. Every method requires a node to interact with its surroundings in order to gather information about its position. Though radio techniques are of most interest, some other communication techniques are mentioned briefly to create a bigger overview. Also, estimated power consumption for the node in each type of architecture and some conclusions are mentioned briefly.

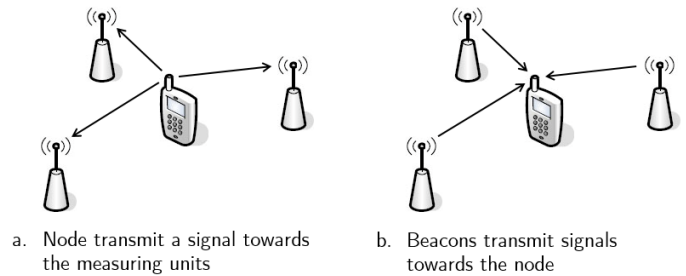


Figure 4.6: Remote positioning (a) and self-positioning (b)

Transfer a signal

The infrastructure from figure 4.6a demands the node to transmit a signal, but it can be very short. The beacons collect this signal and the Central System (CS) contains the Positioning Engine, where the position is calculated. This topology is called **remote positioning** [11].

This technique can be applied in reversed direction as shown in figure 4.6b: when several antennas (e.g. beacons) send a signal towards the node that needs to be traced, it can calculate its position with respect to the sources. This topology is called **self-positioning**: the node functions as its own Positioning Engine. This method demands the node to be receiving radio waves, which consumes less power than transmitting but might require the node to be actively receiving a longer amount of time. If the beacons send an advertisement every second, the node expects that it will have to be receiving half a second before it catches it. Of course, if it knows the pattern of which beacons are transmitting, it can anticipate on when to start receiving. To synchronize the time would create the opportunity to make this method more efficient, but is also another challenge in itself.

With self-positioning, the node can share its position with the CS. This topology is called **indirect remote positioning**. If the position is sent from a remote positioning side to a mobile unit, this case is called **indirect self-positioning**.

Since the CS in most cases knows how to interpret the measurement results better than the node, indirect self-positioning makes more sense. The CS can translate the results for example in symbolic locations like whether the RTI is at a sorting spot or stock.

Note that the RTOF technique for localization is a remote positioning method that requires the node to both receive and transmit.

Collecting reflections

An object can be traced by transmitting a signal to it and collecting the reflections. Examples of this are sonar and radar. Another relatively new method is using multiple antennas: multiple-input multiple-output (MIMO) radar. The reflection method can also be compared with the barcode, which is a method to put information for identification into an optical pattern. A similar method is image recognition as for example with licence plates. This way, both identification and localization can be accomplished, though line of sight is required. There is no known method of mere reflection with

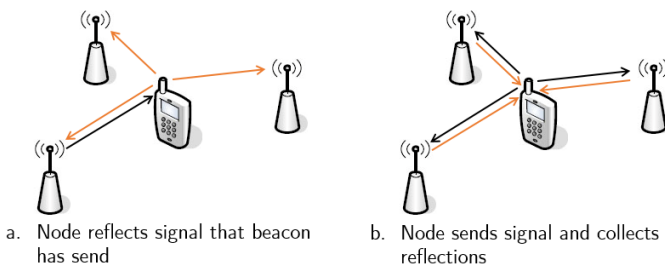


Figure 4.7: Two ways to collect reflections for positioning

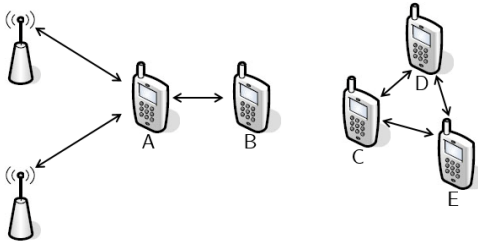


Figure 4.8: Share relative positions through collaboration

radio signals providing both identification and localization. It is also impractical for indoor localization because all the reflections cannot be distinguished.

The same technique as just mentioned can also be accomplished in the reversed direction, like when the node measures the distance to the walls using radiometric, optic or acoustic pulses. This is for example used in robot vacuum cleaners. Information can be gathered about how close the node is to a wall or an object, but not which wall or object (identification).

Collaboration

The above mentioned methods all are beacon based: collecting the location of a node with respect to (static) beacons or anchors with known locations. The computation are carried out in a **centralized** manner: by the CS. In the absence of a CS, nodes can compute their spacing and gain information about their neighbours. The result is a collaborative, **decentralized** method to find relevant information like whether RTIs are positioned among RTIs with the same destination and no stocking conditions are violated. This method is displayed by nodes C, D and E from figure 4.8.

Collaborative positioning requires to be regularly updated and is likely to consume more power. In order to save power, the computations can be **distributed** to minimize communication. This requires the nodes to have some more elaborate intelligence, which is more complex and expensive than individual nodes in a centralized system [15]. An application is also shown in figure 4.8: node A knows its absolute position using the beacons and functions as an anchor node for its neighbours, whether they are within reach of the same beacons or not. The advantage is that only one node needs to be traced (node A) in order to derive the proximity of all its neighbours (node B).

So far, all methods require a form of interaction between the node and surrounding beacons. There is however another asset

that can take over some tasks: equipment like the materials handling. One can think of a forklift or a barcode scanner that performs the positioning (with for example including a view direction and the height that it placed the pallet based on its lifting height) and shares this information with the node and CS. This will minimize the power consumption of the node. This technique will be referred to as the *outsourcing technique* because the node outsources its interaction and computations to the materials handling.

The outsourcing technique can be used additional, substitutional or partially substitutional to the regular technique. A good example is when the CS performs 2-D positioning using the AOA technique. If the forklift is traced and its view direction is known and it shares the height on which it places an RTI, the third dimension is added to the system. It is in this case possible that the forklift maintains the connection with the node so it becomes the gateway of the CS.

C. Localization methodology

We have looked into the architecture, how the components can interact and which component can act as Positioning Engine. Section III-D introduced the properties of waves that enable localization, and has shown the advantages of using radio waves. This section looks at the possibilities to apply localization, identification and communication from the perspective of the transportation process and Business Rules (BRs) within a warehouse (see chapter II). In other words: which methods have most potential for being applied to perform positioning RTIs in a warehouse?

Some first conclusions are drawn before the next chapter elaborates more on the demands and limitations of the preferred positioning techniques.

Each type of infrastructure has up- and downsides. Of course combinations of different methods are also possible, for example applying the collaboration technique when no beacons are nearby. Because the technique of collecting reflections has big limitations, that type of infrastructure is neglected.

One must also take into account that multiple nodes can conflict. With the remote positioning method, a protocol is needed to avoid collisions. If hundreds or thousands of nodes happen to advertise at more or less the same time, their messages will collide and information will be corrupted. However, when the nodes are receiving instead of transmitting, one setup of beacons can serve basically an unlimited amount of nodes at once. As mentioned before, this might have a bigger impact on the power consumption on the nodes or request accurate time synchronization

Another aspect to take into account is that the Central System (CS) would in any case need to know the location of the node. The information needs to be transmitted from the node to the CS which not only requires smart planning in order to avoid collisions, but it also gives the possibility for the CS to compute the location from the source of the messages. The node could have sent a short advertisement instead, unless it contains more useful information to derive the position than can be derived from the advertisements only. For example: the

message can contain information about neighbours or beacons and their relative distance to the node.

The outsourcing technique seems to cope with many difficulties, especially given that it has practically unlimited battery supply. It leads to new questions like how extensive this system should become and whether it is possible to apply it only in the forklift or also in other materials handling or manual scanners. Should it attribute to the positioning system or completely take over several tasks?

A safe conclusion will be that every feasible method requires the RTI to be embedded with a system that can function independently. The addition of beacons and a CS and perhaps “smart forklifts” can attribute to this; the next chapter goes into more detail.

V. INTEGRATION

Now the localization methods have been introduced, it is time to discuss which method is most suitable for the integration with smart pallets.

First thing to notice is that the circumstances in which these pallets end up, are changing all the time. They find themselves in a container, at harbours, in big warehouses with lots of other pallets and possibly smart forklifts, warehouses without any integrated positioning system or they can find themselves returned empty to their supplier. The localization method and the operation mode of the embedded node depends on these circumstances.

To distinguish between circumstances, four **scenarios** are introduced. For each scenario, the pallet should act on a different mode and the positioning method will differ. Though these scenario’s might not be comprehensive, they cover a lot of realistic situations.

A. Localization protocols

This section introduces the scenarios and presents a concept localization protocol for the concerning scenario, for which the properties and metrics might change.

For the communicative hardware, it is assumed that each RTI has a Bluetooth transceiver. It is also assumed that it has a Near Field Communication (NFC) chip. This is not a hard requirement, but it creates several possibilities that might become useful. Furthermore, it is assumed that both the Central System (CS) and the node have knowledge about stocking conditions and the destination of the load.

Scenario 1: smart pallets and CS

Let us first consider a warehouse with CS and a protocol that enables bidirectional communication between node and CS. The CS can communicate with the employee so a connection between the node and employee is unnecessary.

The node is able to detect movement and recognise translations between standing still and being transported. Both events are of interest for the CS so the node will send out a warning signal when it detects movement.

While the RTI is on the move, the CS must be able to trace its path. At suspicious behaviour, the CS can brief the employee. The node does not know which path it should take and which direction it is heading, nor can it communicate with the employee. Therefore, the node is just sending advertisements every four seconds from which the CS computes its absolute position. As mentioned in section III-C, a lower accuracy (say <5 meter) will suffice.

When the node detects that it is put down, it will perform one accurate absolute positioning action. It will transmit a signal to the gateways so that the CS can determine its position with high accuracy (<0.8 meter). It is possible that this signal contains a message with data like the local temperature or how bumpy the RTI was transported. It is unnecessary for the node to know its absolute position, but the CS can transmit valuable information like if it is placed correctly or an error occurred.

In this scenario, the employee identifies the RTI using an optical barcode or NFC. As an addition, it should be possible for the employee to connect to the node and exchange data directly via Bluetooth, instead of via the CS. This is important for the robustness of the system, for example in case the CS is overloaded or out of reach.

Scenario 2: smart pallets without CS

This protocol when there is no CS available will be totally different. There is no case of absolute positioning so the node will only be able to perform relative positioning. Every time the node senses that it is put down somewhere, it should scan for its neighbours. If it has found one or more, they can estimate the distance based on the Received Signal Strength Indicator (RSSI) and share this information so they create a mesh network.

The nodes now form a network and are able to inform each other about relevant changes, in particular when one node appears to have a different destination from those nearby. It is even possible that the meshes form a big network of all the nodes in the warehouse, so features like flooding an important message become possible. If RTIs are placed on wrong spots, near RTIs that might be harmful or if the temperature shifts outside the safe region, the nodes will share this information over the whole network.

The last important feature in this scenario is communication with the employee, who carries a device that connects with the nodes nearby. It receives possibly flooded messages from the network and the order association of the RTIs nearby. Using barcode or NFC it scans one RTI in particular to associate the physical RTI with the Bluetooth connection, before transporting it. The device of the employee shares information with the nodes in its reach like what their destination is, if not known already, and the planned time of departure so they can send a warning if they are not at the place of departure in time. The employee its device shares information with the administrative computer over WiFi, so every RTI can still be traced at their relative position and the progress of the sorting is monitored.

Scenario 3: smart forklifts

This scenario is the same as scenario 1, but with the addition of smart forklifts. The integration of an embedded system in the materials handling like a forklift, creates new opportunities for the localization protocol. The impact depends on the complexity of the system. Three options are treated, ordered in complexity from low to high. The first two are denoted as option 1a and 1b, because the localization methodology are the same as will be explained later on.

Option 1a: the forklift merely sampling heights. This scenario is a warehouse with a CS and a forklift which contains a Bluetooth node. This node has only one task: measuring the altitude of the fork and transmitting it to the CS.

The position of the forklift is traced based on its transmissions, and combined with its identity. The altitude of the forklift its load is corresponded with the RTI that it carries, based on their position. The altitude at the moment when it is dropped, is added as the third dimension for the RTI. This is all performed by the CS.

If any error occurs like when the RTI is brought to the wrong place, it is immediately reported to the employee. There could be a small delay because the exact position of an RTI still needs to be determined after the employee put it down.

Option 1b: the forklift with integrated system. In the previous example, there is still an employee needed with a device that can scan the RTI and retrieve instructions from the CS. In this example, the device is integrated with the forklift (or Automated Guided Vehicle, AGV).

When an RTI is loaded upon the forklift, its NFC chip is scanned to identify the RTI. The forklift retrieves information about the destination of the RTI from the CS. Instructions appear to the driver or get processed by the AGV. The position of the RTI is traced using the fast, 2-D positioning from scenario 1. The altitude of the RTI at the moment when it is dropped, is gained from the forklift before it is added as the third dimension.

If any error occurs like when the RTI is brought to the wrong place, it is immediately reported to the employee.

Option 2: forklift as a gateway and taking over the localization. The next scenario is a warehouse with and a forklift (or AGV) which contains equipment to perform localization and acts as the gateway with the RTIs. There are no other gateways mounted on the ceiling or elsewhere. The forklift is now considered the CS, keeping a connection with the local database via WiFi.

When an RTI is loaded upon the forklift, its NFC chip is scanned to identify the RTI. A short connection using NFC is performed to establish a Bluetooth connection between the RTI and the forklift. The employee or AGV immediately retrieves instructions about the pallet. Continuous-time, accurate 2-D tracking of the forklift is performed and the altitude on which the RTI is placed on a rack, is included as the third dimension. Note that it might be useful to derive the view direction of the forklift to transpose its position into that of the RTI. It is possible to equip the forklift with a directional antenna to detect beacons and their position compared to the forklift.

The feature of having a mobile gateway like this creates a mobile reference point for the positioning of the pallets. The

localization error of the relative position of the RTI compared to the forklift will be small, but the error of the absolute position of the forklift will be determinative.

Because the forklift or AGV takes care of all the positioning, the RTI's node is appointed not to. After the forklift has dropped the RTI at the right spot, the RTI is informed about its symbolic position and its new schedule and the connection is aborted.

One can imagine that this procedure is also applicable with passive RTIs using optical barcodes. A warehouse that integrated this system can use both types of RTIs together and reach the same efficiency as the system with smart pallets.

Scenario 4: in stock or shipment without CS

Consider scenario 2 again. When there is no CS available and RTIs are placed in stock, their composition will probably not change often. The nodes can derive this by logging the changes and perhaps even by deriving that they are placed vertically from each other (they shared RSSI information of their peers). In this case, the nodes save power by maintaining their mesh network connection using a smaller duty cycle (less signals per hour).

The same happens when RTIs are placed in a container for long distance transportation, disconnected from any CS. The ship, truck or train can be localized using GPS, but there is no use of tracking or communicating with the individual RTI. Similar as in the stock, the nodes will automatically generate a mesh network with their neighbours and save their energy by decreasing the duty cycle.

In contrast to when it is in stock, the node senses transportation using its accelerometer when it is being shipped. Based on the characteristics of displacement, the mesh network between nodes and maybe even the reflections of the environment (a metal intermodal container functions as a cage of Faraday), the node distinguishes between stock and shipment. The node acts different in both occasions. In the case of a stock, there is no use of scanning for the availability of a CS. When the node knows it has been shipped, this is different. When the node senses that it is being unloaded from a truck or ship, it will start scanning and advertising and further follow the procedure of scenario 2 or 1.

Based on the schedule of the RTI, there is also the possibility for the node to go completely off-line. This is the case when an RTI is in stock or in shipment and it has no tasks like sensing or logging. Especially when the RTI is returned to the originating facility, empty and without schedule, the node can go into sleep until further notice.

In any case or scenario, also when the node is off-line, it is possible to connect to any node using NFC. The NFC tag is a passive device that is activated by radio waves in close range and can reactivate the node. NFC is used to establish a bluetooth connection on which the schedule, information about what the RTI contains, stocking conditions and the condition of the RTI and its contents can be updated.

B. Localization methods

Considering the protocols from section V-A, there are different localization methods and techniques of interest. Scenario 2 and 4 only have the collaboration method at their disposal. The methods to use for scenario 1 and 3 are more complicated. They are divided as followed:

Fast positioning: tracing a pallet fast, reducing accuracy and power consumption of the node. 2-D positioning is sufficient.

Accurate positioning: accurately derive the position of a target, consuming more time and power from the node. 3-D positioning is required.

Smart forklift integration: the forklift or AGV is responsible for determining the altitude of the RTI (option 1 and 2) and possibly the whole positioning procedure (option 2). In the case of option 1: fast positioning is still required undiminished, accurate positioning is still required for 2-D. In the case of option 2: fast positioning has become redundant, accurate positioning is performed by the forklift instead of the RTI. Considering communication: with option 2, the gateways on the static environment have become unnecessary.

C. Localization techniques

Since the fast positioning and accurate positioning methods have to be developed for the system to function, an applicable technique has to be selected. The collaboration method is disregarded for now. The system must be functioning without the smart forklifts so the elaboration on that addition can be postponed. This section gives an overview of usable techniques and concludes with a suggested technique for both methods. It reflects on the techniques as introduced in section III-E and III-F.

The Bluetooth connectivity protocol is suggested to use for the application. Bluetooth 4.0 LE (Low Energy) and later versions are optimized for the purpose of transferring data and creating a point-to-point, mesh or star network. The range is up to 100 meter, which is suitable for indoor, and devices can be localized with an accuracy of up to 0.4 meter [27] using RSS.

It might be considerable to use TDOF or AOA localization techniques, or a hybrid system of those, in order to gain a higher reliability. Those techniques have other up- and downsides. The following overview is explained in more detail in [15].

RSS localization is a cheap and easy technique to apply. It is however not the most accurate and easily affected by obstacles and multipath components. The authors of [28] performed indoor BLE RSSI positioning in four stages. The stages include modelling RSSI values, decreasing the sampling errors by smoothing the received RSSI, positioning using a cooperative localization method and finally, adjusting the model based on results. These adjustments are very important in a warehouse where the circumstances change by the minute.

Scene Analysis (SA) can partially solve the inaccuracies: the node's RSS values of its neighbours can be shared to obtain a fingerprint of the node its surroundings. It is possible

that these are indeed its neighbouring nodes, like the mesh network as elaborated in scenario 2 which requires a lot more power consumption, but they can also be beacons. If large amounts of those are installed close to the ground, emitting an advertisement every second with the same power, the node can collect those with their RSS value and create a fingerprint. An illustration of this method is given in figure 5.9. The advertisements can also contain information like its symbolic location.

TDOA does not require time synchronization between transmitters and receivers, but only between the receivers. This requires expensive equipment, especially for large deployment. It is however robust against multipath and NLOS (No Line of Sight) and provides centimeter level accuracy.

AOA can achieve similar accuracy and is also robust against multipath. It is however infected by NLOS conditions and requires special equipment.

The authors of [29] introduce a hybrid of TOA and AOA, which is robust against NLOS and multipath. It is however way more complex than TDOA only and not suitable for our case.

Another possibility is to use acoustic waves. The TOF can very easily be measured compared to a radio wave, so the distance can be derived. Some downsides are: it requires new equipment, it is slower so the chance on collisions increases and there is no optimal frequency. Low frequencies are audible and might disturb people. They also need bigger sound boxes and more power. High frequencies or ultrasound waves do not diffract very well and get absorbed easily when they penetrate objects. LOS is required or only reflections are caught by the measurement device, giving a false indication of the distance.

As for the forklift integration, the technique will differ as follows. In case of option 1, the localization technique will be exactly the same. The sampling of the height that is performed by the forklift, will be added to the system. It can be used complementary to the 3-D positioning technique, or added as the third dimension to the 2-D positioning technique. In case of option 2, the forklift becomes the mobile target that has to position itself. As mentioned in section IV-C, it leads to several new opportunities, applications and questions on how to implement it. It would be too extensive to treat that subject full-fledged in this paper. In short, the fast positioning technique is cancelled because the static gateways are left out. The forklift has enough battery capacity to perform Scene Analysis and perhaps new techniques like Dead Reckoning constantly. It can position an RTI based on its own position and view direction and the height on which it places the RTI.

Considering the techniques to use for sampling the height, there are also multiple techniques. For example: measuring the air pressure very precisely, measuring acceleration or by measuring the distance to the ground using ultrasound waves. This new equipment can be applied to the forklift, as mentioned before, but also to the RTI.

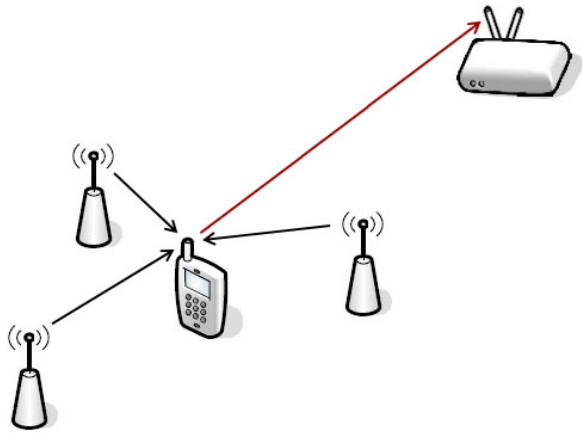


Figure 5.9: Accurate positioning using Scene Analysis

Conclusion

The TDOA might perform best for the implementation of accurate positioning because it is the most accurate technique and robust against NLOS and multipath propagation. It however requires very special equipment and very precise time synchronization. The complexity of this system might be a stimulant to implement a more simple and possibly cheaper one. In this case, it is proposed to use two separate techniques for the fast and the accurate positioning methods.

The Scene Analysis method has a lot of potential for *accurate positioning*. Beacons can provide high accuracy and gateways can collect fingerprints from the nodes. This technique might be more feasible than TDOA. An illustration of what is meant with the SA method is displayed in figure 5.9: the mobile device measures the RSS of three beacons and transmits the measurement towards the gateway.

For the *fast positioning* method, this technique is not useful: the composition changes while the node is measuring for beacons nearby. Positioning the target with gateways using the RSS might reach sufficient accuracy. It remains unclear how accurate this will become since the ceiling can be very high. The accuracy decreases exponentially with the height of the measurement antennas, and is severely influenced by NLOS. The angulation method could perform better, but at least be easily implemented in addition to the lateration method. If two or more gateways are able to determine the RSS and AOA from a mobile target, the position can possibly be determined with a high accuracy, consuming little time and energy.

If this works as suggested, it is a system that fully complies with scenario 1.

VI. RESEARCH SCOPE

The positioning system as described before, would be a very interesting methodology to implement and perform a research about. It contains the accurate positioning using fingerprints (Scene Analysis), the fast and low-energy positioning using RSS, the addition of AOA information to improve the fast localization and possibly the addition of smart forklifts.

The third subject of this enumeration – the addition of AOA information – especially gained attention. This section explains why and what the scope of this particular research will be.

A. AOA: added value

The use of SA and lateration using the RSS is a widely used technique. The addition of deriving the AOA to improve the localization accuracy is however not very widely known. The information about the AOA is therefore often disregarded, which would be a waste if this information can improve the accuracy significantly and is worth the cost in special equipment and implementation effort.

This specific element is therefore subject in the further research of this paper. Knowing the technologies to derive the AOA, how to use it, how accurate it is and how this accuracy is influenced by the environment forms a piece of the localization technique and methodology that can be applied in the protocols that have been introduced before. It can be used in addition to the lateration technique, implemented in gateways spread over the ceiling, build onto possible smart forklifts or it can be used for numerous other localization purposes.

The rest of this paper restricts to the subject of deriving the AOA, leaving the implementation of it to future study. The research questions will be as follows:

What are possible current known technologies to determine the Angle Of Arrival from a radio signal? Which technique has the most potential to be applied in the positioning of pallets in warehouses? How accurate is this technique in determining the Angle Of Arrival, what are the sources of inaccuracy and how big is their influence?

With “current known technologies”, also the current used hardware is meant: no hardware is designed or altered for this research. The “radio signal” has later in this paper come down to specifically Bluetooth Low Energy (BLE) signalling only, leaving other radio communication means disregarded.

The first two questions are treated in the next subsection and come to a research about the third question in the following section.

B. Current Angle Of Arrival Systems

There are typically two types of equipment to determine the AOA: array antennas and switched-beam antennas [11, 15].

An array antenna contains two or more antennas that are very close to each other. Instead of RSS, they have to measure the difference in phase of a wave coming from a transmitter to determine the AOA [30]. In short: if one antenna is one fourth of the wavelength closer to the source, the phase will be one fourth of the wavelength ahead of the other antenna. This is comparable to the TDOA-technique, but then on a very small scale. With the antennas being so close to each other, no separate devices with intensive time synchronization are required. Because of multipath propagation and fading, determining the AOA using an array antenna is a bit more complicated than just measuring the phase difference. There

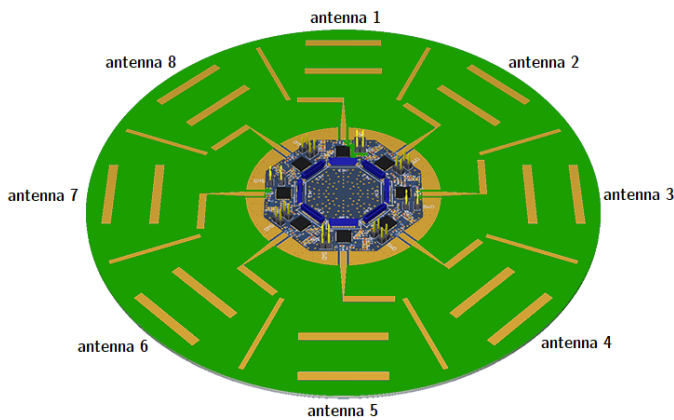


Figure 6.10: PCB and antenna layout

are multiple estimation methods to accomplish this. Some of them are: Estimation of Signal Parameters via Rotational Invariance Techniques (ESPRIT) [31], Multiple Signal Classification (MUSIC) [32], Conjugate Augmented MUSIC (CAM) [33] and Time-Reversal MUSIC (TR-MUSIC) [34]. A Multiple Antenna System (MAS) like this is difficult to apply on a large scale network of nodes because there is a substantial hardware requirement of these schemes [35]. It is easier to apply on anchor nodes which than can feed back their measured AOA to the mobile nodes [36]. It is also possible to derive the Angle Of Departure from a MAS anchor node: the authors of [35] introduced a distributed angle estimation using a two-antenna anchor. By emitting two linear chirp waves with slight frequency difference, an interference field is produced. The RSSI of these signals is captured by sensors to estimate the AOD and so derive its relative location.

Switched-beam antenna systems are less complex: they make use of directional antennas and correspond the RSS with a certain direction to determine the AOA. It can for example be a rotating dish antenna that collects samples from all directions. Another directional antenna like a Yagi antenna can be used, and it can be multiple fixed antennas instead of one rotating antenna. The authors of [37] performed this principle with a directional anchor antenna on the ceiling to enable indoor 2D target positioning by sensor nodes. The authors of [38] obtained the AOA by measuring the RSS of a rotating anchor node [39].

The switched-beam antenna does not need complex estimation methods and can be very simple to manufacture. A good example is the one displayed in figure 6.10. Eight Yagi antennas are mounted on fixed positions on this Printed Circuit Board (PCB). They can individually be controlled by a source or, as in this case, have NRF52832 Bluetooth modules mounted to them. These chips can individually be programmed to transmit signals or measure the strength of received Bluetooth signals of their own direction. This particular model has a lot of potential to perform angulation and can be manufactured for large scale use. It has however not been extensively tested before, so the next chapter will gain new insight on how this device can be used to derive the AOA.

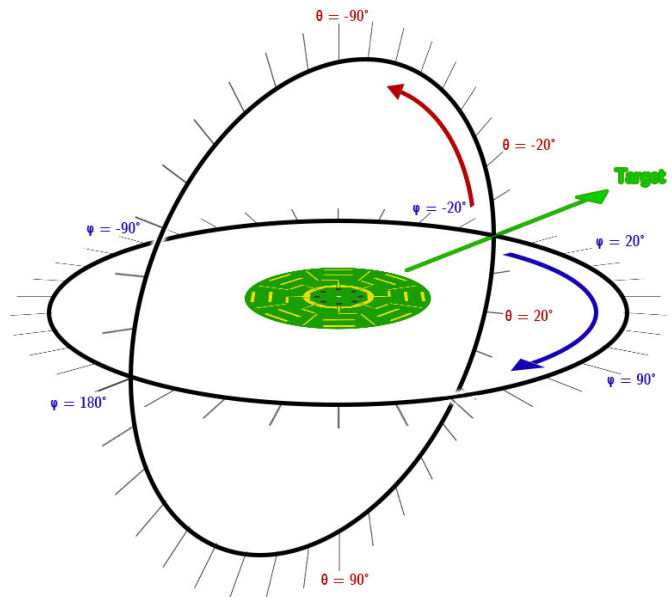


Figure 7.11: Orientation of the PCB compared to the target

VII. RESEARCH: SWITCHED-BEAM SYSTEM TEST

The printed circuit board displayed in figure 6.10 contains eight directional antennas, placed in directions that are 45° apart. In this paper it will be referred to as *the PCB* (Printed Circuit Board). Depending on the distribution of measured values from these antennas, the PCB can perform angulation to recover the direction of the target to be localized. How to do this, is the main question of this research. The behaviour of the antennas in all directions must be evaluated in order to find sources of inaccuracy and how big their influence is on determining the AOA.

Several test have been performed. A big part of this was inside an anechoic chamber, to find the sources of inaccuracy on the smallest scale without reflections influencing the behaviour. This gave a shape of the transmission of one antenna and three models of how the composition of antennas receives the signal from a target on different altitudes. A converter is build to convert one measurement into an estimated AOA. This system is then evaluated and multiple sources of inaccuracy get uncovered. Finally, the effects of polarization and reflections in a realistic indoor environment are shown to decrease the accuracy of the system so much that the models from the anechoic chamber are inadequate.

Each antenna has its own MAC-address. For convenience they are named “antenna 1” up to “antenna 8”, clockwise, where antenna 1 is the reference point. In other words: antenna 1 is located at 0° , antenna 2 is located at 45° and so forth, as displayed in figure 6.10.

The PCB needs to be tested in two different angles: horizontally and vertically. The rotation of the PCB with respect to the target is used to define these angles, where ϕ (phi) is the clockwise horizontal rotation and θ (theta) is the

vertical tilt. Figure 7.11 shows how this is organized. $\theta = 0^\circ / \phi = 0^\circ$ means that the PCB faces the target with the primary antenna. The ϕ -angle and θ -angle represent the rotation of the PCB from this point. If ϕ increases, the PCB is rotated clockwise. If θ increases, the PCB tilts over so the target is orientated towards the top of the PCB. θ goes from -90° to 90° (where the target is located perpendicular to the bottom and top of the PCB, respectively), while ϕ goes around from -179° to 180° .

Depending on the orientation of the PCB, a different signal strength is expected at each antenna. Based on the distribution of these values, the direction of the target can be determined. Logically, the antenna that is directed most closely to the target is expected to gain the highest Received Signal Strength.

This description gives the impression that the PCB is the measuring device, receiving the signal from the target as a source. In practice, this measurement can be performed in both directions: the PCB can emit the signal and the target can measure the signal strength of these eight transmissions.

Test setup

The PCB is tested in an anechoic chamber, on a setup as displayed in figure 7.12. The PCB is connected to a PVC rod, together with a compass card that is laser cut from a triplex board. The PCB can be rotated and the compass can be used to determine its ϕ -rotation, accurate within less than a degree.

The rod is held at place with PVC tubes, and connected to a stepper motor that can make steps of 1.8° (200 steps in a full rotation). This is the θ -rotation.

Notice that the test setup in figure 7.12 is not oriented straight. Turning the picture clockwise a quarter shows how the data should be interpreted: with the right wall being the downside.

The PVC of the stand has a very small influence on the radio propagation, which is neglected for this research. The stepper motor has a bigger influence on the radio propagation, but this is minimized by placing it one meter from the PCB and adding the Styrofoam peak that covers it.

The target is a USB dongle. It is taped to a wooden stand and connected via a cable to a computer outside the room.

All the tests are conducted with a constant distance of 240 cm between the dongle and the center of the PCB.

A. Test 1: PCB / Dongle measurements

The first test shows the difference between the measurements performed by the PCB (collecting signals from the dongle) and those performed by the dongle (collecting signals from the PCB). The PCB is placed at $\phi = 22.5^\circ$, a test is performed to collect around 250 samples, the PCB is rotated 45° , and the same test is performed until all eight antennas have covered all eight positions (with $\theta = 0^\circ$). Each antenna now delivered an average and a standard deviation of around 250 RSSIs (Received Signal Strength Indicator). The average of these eight averages is calculated and displayed in figure 7.13. Also the average of standard deviations is displayed in the graph as the error



Figure 7.12: Test setup

bar. Note that these standard deviations are not the same as how far the averages of the eight antennas are actually apart.

From the results can be seen that the results are very similar, but have an offset of approximately 5dB. Because for the calculation of the AOA (Angle of Arrival) only the distribution of the RSS over the eight antennas is relevant, the absolute RSS value and offset of the graph is irrelevant. Both graphs lead to a peak at $\phi = 0^\circ$.

From now on, for the ease of the conduction of the tests, only the dongle is used to perform measurements.

Furthermore, the graph does not show that the antennas are quite similar above $\phi = -22.5$ but differ a lot at $\phi = -67.5$ and $\phi = 112.5$. Figure 7.15 will confirm that the antennas give very different results around $\phi = -90^\circ$. This is likely to be caused by small differences in the hardware.

B. Test 2: elaborate 360° rotation measurements

The graphs from figure 7.15 show two different perspectives of the PCB.

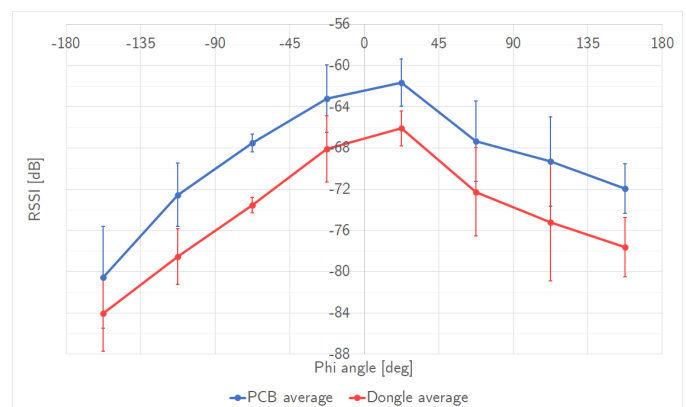


Figure 7.13: Measurements from the PCB compared to those of the dongle

The first one is the average of averages. It is similar to the one from test 1, only now it is conducted each 22.5° instead of 45° . The graph shows the average of all the antennas (eight times 200-300 samples). The error bar is now the standard deviation between the eight antennas. At $\phi = -90^\circ$, the differences between the antennas run apart severely. The dotted line in between show an estimation of this average: a curve computed as a hermite spline. This curve is considered to be the model of ϕ at $\theta = 0^\circ$ from now on. The error bars represent the standard deviation of the curve, based on the mutual difference of the reception the antennas (later referred to as “mutual deviation”).

The second perspective is the series of 10 measurements with a resolution of 5° , conducted by all eight antennas at their own region. They are displayed in the vivid graphs, accurately following the curve mentioned before.

Two distinct lobes (peaks) become clear: one at 0° and one at 90° . Similar to the previous test, the area around -90° contains smaller lobes that differ with each antenna.

C. Test 3: evaluation of theta

One might assume that the model that was obtained from $\theta = 0^\circ$ (the curve from figure 7.15) is similar for all θ , only that the intensity increases or decreases until they reached an equilibrium at both $\theta = 90^\circ$ and $\theta = -90^\circ$. In reality, the influence of the tilt is way more complex than that.

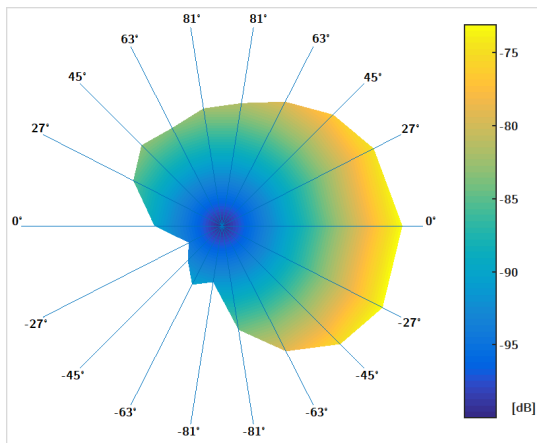


Figure 7.14: Vertical crossview: viewing rotation of θ at $\phi = 0^\circ/180^\circ$

Figure 7.14 shows the crossview of the lobe at $\phi = 0^\circ$ and the other side: $\phi = 180^\circ$ (measured by antenna 8 only). It reveals the asymmetry of the up and downside of the PCB. The models for $\theta > 0^\circ$ and $\theta < 0^\circ$ will differ.

Figure 7.16a and 7.16b show that also the horizontal shape transforms, rather than reaching an equilibrium. The shape of the model from figure 7.15 is visible in the dark graphs. The lighter graphs show that the side lobe (at $\phi = 90^\circ$) increases and eventually transcends the main lobe at negative θ . At positive θ , this side lobe decreases but a stronger lobe at $\phi = 180^\circ$ starts to arise. It appears that different models are required to compute the ϕ -angle, based on the θ -angle. This is very unfortunate

since both variables are unknown in most cases of application.

Figure 7.17 and 7.18 show a 3D-model of the emission or reception of one antenna. Note that:

- It shows emission power in pW, instead of dB. This gives a more exaggerated view.
- The data is mirrored: ϕ has shifted positive and negative. This shows the true radiation pattern instead of the reception based on the rotation of the PCB.
- The area around $\theta = 90^\circ$ and $\theta = -90^\circ$ is unpredictable and influenced by the polarization of the signal (as will be explained later). In order to prevent holes in the model, arbitrary points are drawn in the middle of both the up- and downside that close the connection.
- The same data as from figure 7.16a and 7.16b is used. It is gained from eight antennas that each cover an area of 45° .
- $\theta = -27^\circ$ has outliers at $\phi = 10^\circ$ and $\phi = -35^\circ$ (and some other multiples of 45°) which are unreliable. These have been suppressed.

D. Converting measurements to angles

This section shows how the model is used to compute the estimated Angle of Arrival from several measurements. The model is made from the sixteen values from $\theta = 0^\circ$ and the curve that is drawn in between, as displayed in figure 7.15.

This curve is computed as a hermite spline between the reference points. The curve that represents the Standard Deviation of the model is computed the same way. Both the model and its Standard Deviation are displayed in figure 7.19.

To compute the angle from one measurement, it is compared to the model. One measurement contains eight values, one from each antenna (which is an average of approximately 250 samples). These values are “swiped” over the model, like visualized in the green graphs from figure 7.19. The rate of deviation from the value to the model, is expressed as a multiple of the Standard Deviation. If the value is the same as the model, the rate is 0; if the value is one Standard Deviation away from the model, the rate is 1. In this way, each value is rated for each reference point of the model. Then, the average of all these rates is computed. The place where this is the lowest, must show which angle from the model corresponds best with the measurement.

Figure 7.20 shows how this computation looks like. The top row shows the angle of the reference spots (it shows only 16 references to the model, but in reality 64 were used). The rows below show the rate of deviation for each antenna. The row at the bottom shows the average where the lowest is coloured green. In this case the measurement is corresponded with the angle of $\phi = 45^\circ$, where each antenna was about one SD away from the model on average.

The green graphs from figure 7.19 correspond with the columns of 0° , 45° and 90° from the table in figure 7.20. The current table can compute the ϕ -angle of a measurement in steps of 22.5° . The model with 64 reference points can bring this down to 5.625° . Increasing the number of reference points will increase the resolution. There is also another way

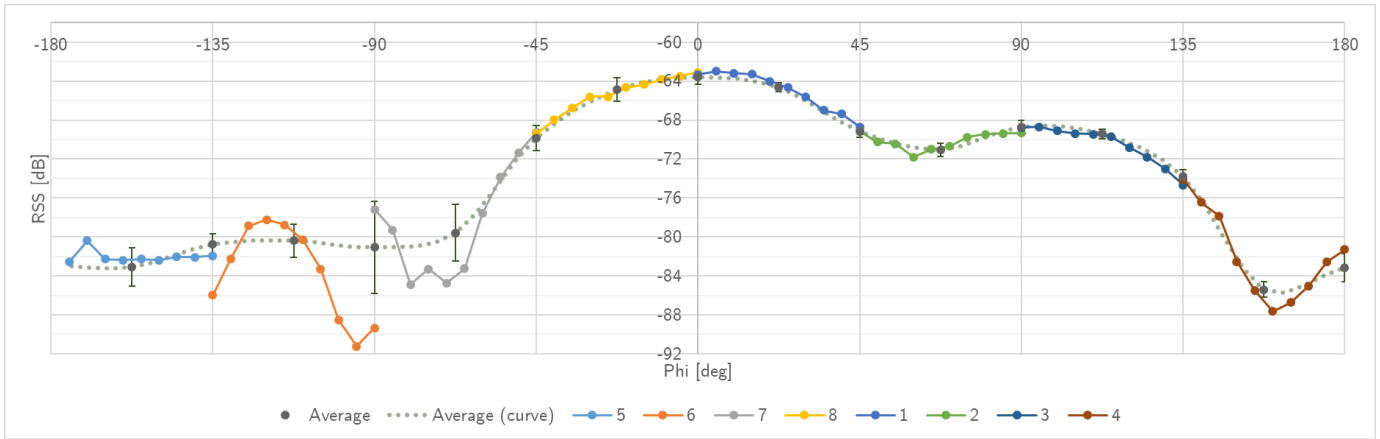


Figure 7.15: Rotation of ϕ around 360°, $\theta = 0^\circ$

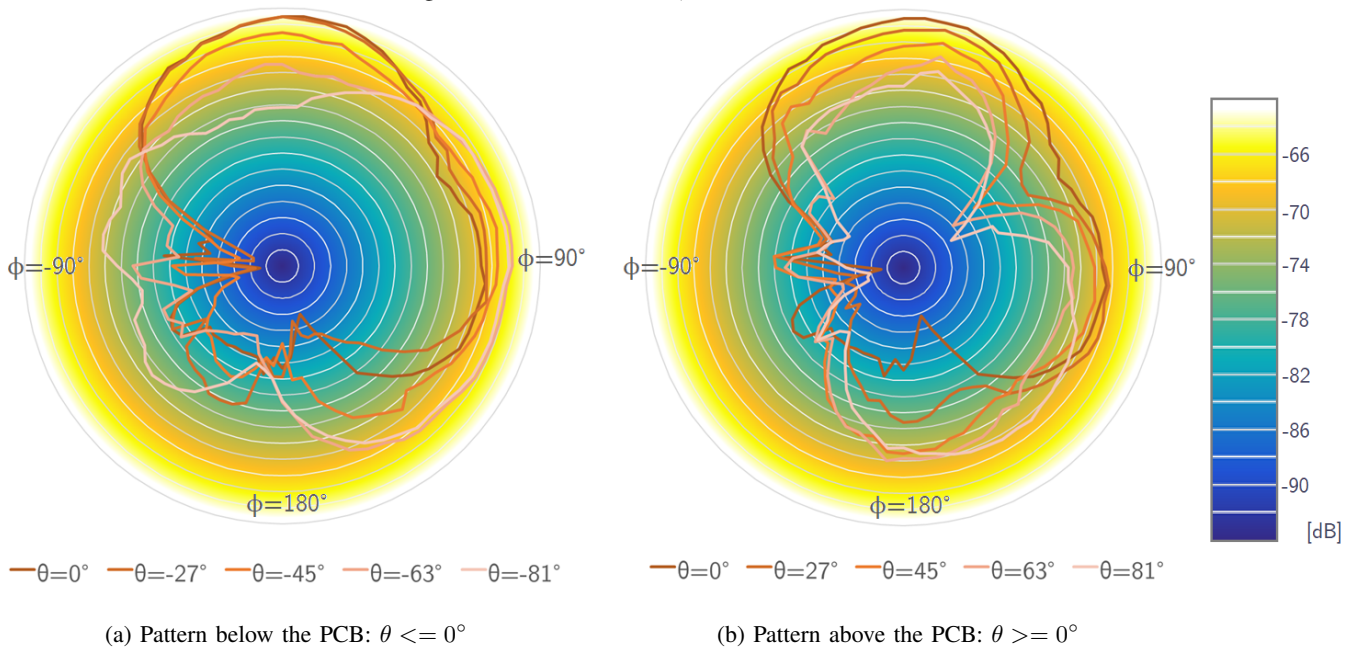


Figure 7.16: Horizontal crossview, divided in the bottom side and top side of the PCB

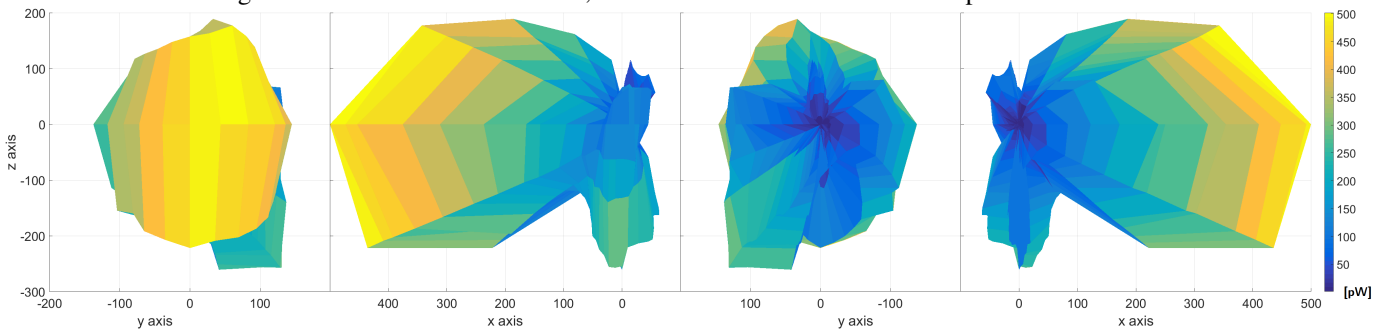


Figure 7.17: Side view of the 3D-model from four different angles

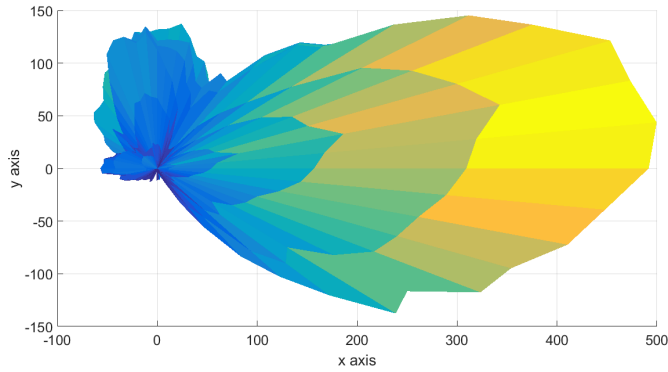


Figure 7.18: Top view of the 3D-model

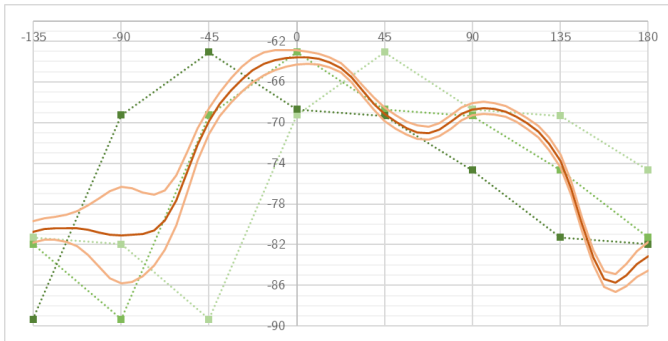
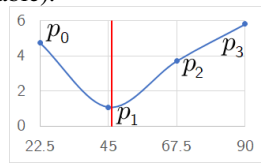


Figure 7.19: Model including Standard Deviation. The three green lines are comparisons of one measurement with the model.

to estimate the angle between two reference points and that is by computing the top of a virtual curve between the rates (the red-green coloured boxes from the table).

An easy computation to estimate the position of the top between two points, is $\frac{p_2 - p_0}{p_1 - p_3 + p_2 - p_0}$ where p_1 and p_2 are the lowest adjacent points and p_0 and p_3 are the points next to them. The result is a value between 0 and 1, corresponding to the estimation of the top between p_1 and p_2 . Applied on the previous measurement, the result was 45.30° . This means that the model estimation was 0.3° off from the real value.



The accuracy of the converter can now be evaluated, but it would be based on one steady signal strength. In reality there would be an offset of the measurement's received signal strength, depending on the distance to the source. How this calibration can be performed is explained shortly, but first some evaluation on the overall received signal strength.

E. Proximity based on RSS

The distance between transmitter and receiver can be estimated by knowing the difference in signal strength and using the Path Loss formula. For this, you need to know the Path Loss Exponent (PLE) [40]. In an indoor environment, this can easily vary between 1.5 and 3 (depending on whether there is

Model $\theta = 0^\circ$											Deviation from model					
	-158	-135	-113	-90	-68	-45	-23	0	22.5	45	67.5	90	113	135	158	180
0	7.3	11.4	6.8	2.6	3.7	0.9	3.2	7.4	8.9	0.7	3.6	0.0	1.4	7.8	21.4	10.2
45	6.4	2.5	3.5	0.4	3.7	8.3	10.2	0.3	2.6	1.0	0.2	6.9	20.6	9.7	7.0	10.8
90	1.7	3.8	8.1	16.0	21.8	8.6	5.6	9.6	10.6	1.4	13.8	6.0	4.3	5.8	3.3	1.3
135	13.5	25.6	36.2	19.0	15.8	20.2	24.0	11.6	5.3	1.3	0.9	0.5	0.5	0.0	0.6	9.0
180	37.7	20.0	16.8	21.2	25.4	12.6	4.4	0.8	0.6	1.1	0.9	0.2	0.8	9.5	14.1	26.6
-135	28.1	33.1	40.3	24.0	5.0	4.4	3.2	8.1	5.2	1.7	3.3	15.3	20.2	37.3	53.7	31.6
-90	0.3	7.0	20.7	9.8	7.0	10.9	6.5	2.5	3.5	0.5	3.6	8.2	10.1	0.2	2.7	0.9
-45	28.6	14.1	10.2	16.8	10.1	3.8	5.6	5.3	1.5	0.7	3.4	9.5	12.3	9.0	12.8	16.5
	15.5	14.7	17.8	13.7	11.6	8.7	7.8	5.7	4.8	1.1	3.7	5.8	8.8	9.9	14.5	13.4

Figure 7.20: Table that shows a computation of the angle based on 16 reference points.

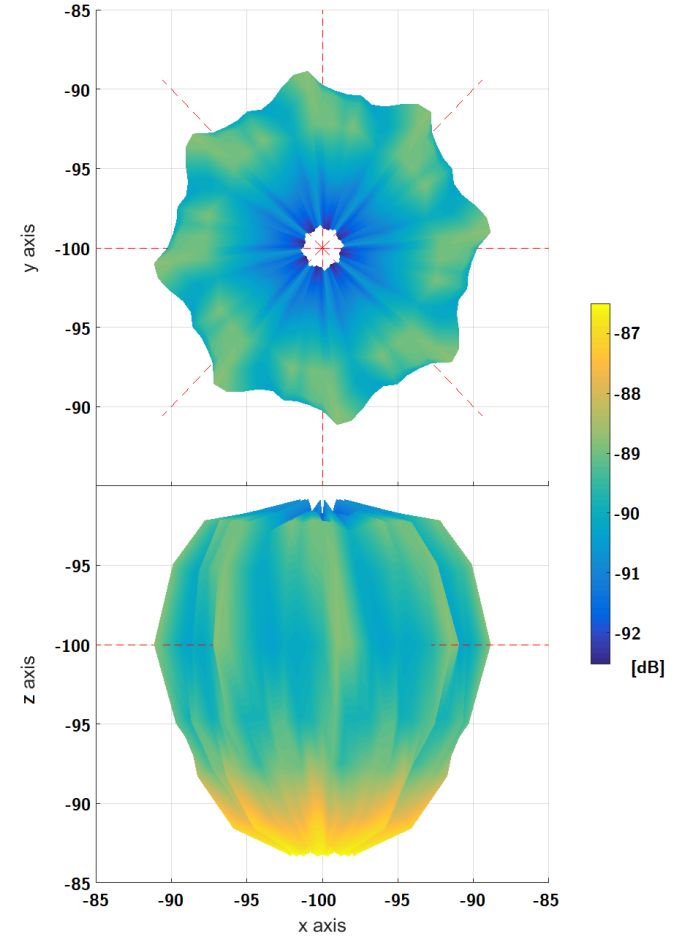


Figure 7.21: Signal Strength – the average of all eight antennas.

LOS or not). For the sake of this example, a PLE of 2 is used (which corresponds to free-space path loss, like expected in an anechoic chamber). This means that the signal strength drops with the distance squared: at 20 meter, the signal strength would be $\frac{1}{4}$ of the signal strength at 10 meter from the source. This equivalent to -6 dB.

In practice, the signal would be distorted by all kinds of fading. This will have its influence on the angle measurement, but even more on the the estimation of the distance based on the Received Signal Strength (RSS). The accuracy depends on the estimation of the PLE for the respective environment [41].

Furthermore, it is difficult to obtain the signal strength from directional antennas. One way is to take average of all eight antennas, but still the result will differ depending on the angle of arrival. The reception on the horizontal plane ($\theta = 0^\circ$) fluctuates 1.6 dB and the reception on the bottom (around $\theta = -81^\circ$) is up to 6 dB higher than at the top (around $\theta = 81^\circ$). The Signal Strength, based on the average of all eight antennas, is visualized in dB in the model from figure 7.21. The direction of the antennas are drawn as red dashed lines. The top and bottom of the model are left open because there is no data for those spots. The scale is put in dB, where -100 dB is the lowest.

F. Calibrating signal power

To estimate the Angle of Arrival, the reference point from the model that fits best to the measurement is computed. In this computation, only the relation between the eight antennas is relevant. The strength of the signal is not relevant to determine the AOA. Therefore, the eight samples can be provided with an offset. This might calibrate the measurement so that it fits best to the reference points. This way, the best corresponding angle can be computed for any distance to the target (or other influences that affect the signal strength).

The calculation of the rate is explained before in section VII-D, its equation looks as follows.

$$r = \sum_{n=1}^8 \left| \frac{\Delta_n}{\sigma_n} \right| \quad (1)$$

In this formula: r is the rate, n is the antenna in question, Δ is the difference between the measurement sample and the model and σ is the Standard Deviation of the value in the model (also referred to as the “mutual deviation”).

An offset x can be added to the measurement samples Δ_n . The rate is the sum of deviations as absolute values, but it does not tell whether the total deviation is overly higher or lower than the model. Since the total deviation needs to be as small as possible using the offset, the absolute value brackets are removed.

$$\text{total deviation} = \sum_{n=1}^8 \frac{\Delta_n + x}{\sigma_n} = \sum_{n=1}^8 \frac{\Delta_n}{\sigma_n} + \sum_{n=1}^8 \frac{x}{\sigma_n} \quad (2)$$

The offset x needs to be chosen so that the this total deviation becomes zero. By rewriting the formula, we can obtain an equation to compute x .

$$x = - \frac{\sum_{n=1}^8 \frac{\Delta_n}{\sigma_n}}{\sum_{n=1}^8 \frac{1}{\sigma_n}} \quad (3)$$

Adding the offset x to the computation of the rate, shifts the measurement up or down so that the rate becomes as small as possible.

This system works and makes the system more robust against change of signal strength, but it might also decrease the accuracy a little: when the distance to the target and therefore the signal strength is known, like in the test setup, the measurement should not be shifted to fit best to every possible angle. It might occur that due to noise – the small

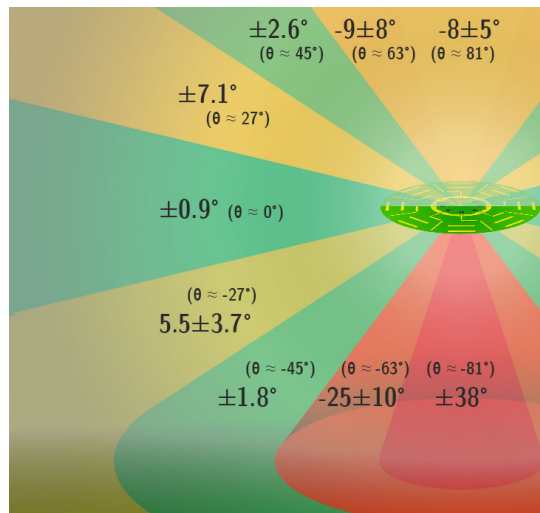


Figure 7.22: Accuracy of the current method illustrated.

Table 7.1: Accuracy of the current method.

	Average rate per model				Average ϕ -error
	-45°	0°	45°	score	
$\theta = 81^\circ$	5.5	4.7	3.3	90%	$\pm 9.9^\circ$ or $-8.1 \pm 5.4^\circ$
$\theta = 63^\circ$	5.4	4.5	2.1	90%	$\pm 11.0^\circ$ or $-9.0 \pm 7.9^\circ$
$\theta = 45^\circ$	3.9	4.1	1.0	60%	$\pm 2.6^\circ$ or $-1.2 \pm 2.6^\circ$
$\theta = 27^\circ$	2.6	2.6	2.8	40%	$\pm 7.1^\circ$ or $0.8 \pm 7.1^\circ$
$\theta = 0^\circ$	2.9	1.1	5.0	100%	$\pm 0.9^\circ$ or $0.0 \pm 0.9^\circ$
$\theta = -27^\circ$	3.2	1.9	5.5	70%	$\pm 5.6^\circ$ or $5.5 \pm 3.7^\circ$
$\theta = -45^\circ$	1.0	1.9	4.2	80%	$\pm 1.8^\circ$ or $0.0 \pm 1.8^\circ$
$\theta = -63^\circ$	3.0	2.8	4.8	20%	$\pm 30.5^\circ$ or $-25 \pm 10^\circ$
$\theta = -81^\circ$	3.6	3.8	3.8	20%	$\pm 37.6^\circ$ or $-0.6 \pm 38^\circ$

deviations within antenna measurements – the sample fits better to another angle due to this offset. It appears that this is indeed the case for some tests (see table 7.2), though the influence is small.

Because it is assumed that the true signal strength is unknown in practice, it is better to still take the automatic generated offset into account.

This offset can be used to estimate the distance to the target: if the offset is 0, the distance to the target would be close to 240 cm. If the offset is 3, the distance would be 480 cm.

G. Determining the accuracy of the system

The system that is created to estimate the Angle of Arrival based on measurements can automatically create a signal strength offset for the measurement, compare it to models and rate its conformity, pick a model and compute the estimated AOA based on the rates.

The three models that were used, are based on the reception at $\theta = -45^\circ$, $\theta = 0^\circ$ and $\theta = 45^\circ$. Using these models, the system was able to determine the AOA with an accuracy around 2° at the corresponding tilts. At different tilts, the system performs a lot worse. The performance is displayed in figure 7.22, and more elaborately in table 7.1.

The data is based on ten real measurements ($\phi = 0^\circ$ to $\phi = 45^\circ$ in steps of 5°). The average rate of these measurements per model is displayed in the table, where the rate of the dominant model is made bold. This means that the model had the lowest

rate for at least 8 of the 10 measurements. It appears that there is no dominant model at $\theta = 27^\circ$ and $\theta = -81^\circ$.

The score means how often the model with the lowest rate was actually the one with the best accuracy. The model that fits best to the measurement based on rate, is only in approximately 65% of the cases the most accurate one. The model of $\theta = 45^\circ$ had for example a low score at $\theta = 45^\circ$, while its rates were by far the lowest. Partially, this can be explained as coincidence. For example: at two of these measurements, model $\theta = 0^\circ$ made a very accurate estimation (0.3° and 0.2° error) while it had bad estimations at other measurements.

The overall accuracy of the system is given in the right part of the model. The average ϕ -error is given both without and with a shift to display precision and accuracy. A weak point of this test would be that the measurements were only from $\phi = 0^\circ$ to $\phi = 45^\circ$. A better validation would have been to take random points within 360° . The next section realises this in a more accurate, virtual test on the model-specific θ -angles.

When looking back to figure 7.16a (p. 17), it appeared that the main lobe lost strength at $\theta = -63^\circ$ and $\theta = -81^\circ$ while the strength of the side lobe increased. The result is that the model $\theta = 0^\circ$ repeatedly estimates the AOA at around $\phi = -40^\circ$ (7 out of 10 measurements had an error between -32° and -44°). This happens also at other tilts and demonstrates the mutation of the model over different tilts. With a different model, the angle can still be computed at $\theta = -81^\circ$.

When the PCB is hung up near the ceiling, only the top or bottom side is used to determine the AOA. Since the top side of the PCB performs better with the current system, as can be seen from figure 7.22, it would be in favour to use. However, this difference can be decreased by creating new models for the top and bottom region. There is however another advantage of using the top side of the PCB instead of the bottom side: with the current models, the rates are on average higher at the top. A new model in that region would be less confused by the current models than it would on the bottom side because the shape differs so much. But this is just hypothetical, the models need to be designed and tested to show if that is true or if there is another reason why it would perform less good. Both regions seem to have quite a distinct shape, as can be seen in figure 7.16 (p. 17), so the rates will probably differ enough too.

There is another reason to choose for the bottom side: the reception is better. This follows from the graphs of figure 7.16 and section VII-E. This might turn out to give an advantage in computing the AOA, for example with weaker signals.

H. Inaccuracies uncovered

In section III-D (p. 5), large scale fading and small scale fading have been introduced. These disturbances will influence the reception and computation of the Angle of Arrival. Within the anechoic chamber, the environmental conditions that influence the accuracy are brought to a minimum. This way, other sources can be investigated.

In section VII-G, in figure 7.22, the accuracy of the method from three models is displayed. This section is to make an

Table 7.2: Values of inaccuracy in determining the AOA.

	Average ϕ -error		
	Converter	Antenna (mutual)	Antenna (internal)
$\theta = 45^\circ$	$\pm 1.33^\circ$	$\pm 1.35^\circ$	$\pm 6.67^\circ$
Without AGO	$\pm 1.25^\circ$	$\pm 1.60^\circ$	$\pm 8.22^\circ$
$\theta = 0^\circ$	$\pm 0.37^\circ$	$\pm 1.66^\circ$	$\pm 3.34^\circ$
Without AGO	$\pm 0.36^\circ$	$\pm 1.21^\circ$	$\pm 3.94^\circ$
$\theta = -45^\circ$	$\pm 0.48^\circ$	$\pm 1.54^\circ$	$\pm 3.87^\circ$
Without AGO	$\pm 0.49^\circ$	$\pm 1.30^\circ$	$\pm 4.28^\circ$

overview of all the inaccuracies that emerge between the transmission of signals and the computation of the AOA, that can be quantized based on the experiment results.

All the inaccuracies are considered to be normally distributed random variables. The values are expressed as average error in determining the ϕ -angle in degrees. In most cases, this is the same as the average error like used in figure 7.22 and table 7.1. This value is close to 80% of the Standard Deviation. In the case of the target orientation, the error is expressed as a shift and an average deviation.

The values displayed in table 7.2 are typical deviations, caused by limitations of the hardware and type of conversion. They are tested with and without Automatically Generated Offset (AGO), to show the effect of this feature that was explained in section VII-F (p. 19). As shown in the table, it can both increase and decrease the error. Because the signal strength is said to be unknown, the AGO should be included by default.

The converter is the part of the method to pinpoint the AOA by comparing it to the model using 64 reference points (as displayed in figure 7.20, p. 18). The weak part of this technique is the determination of an angle between two reference points, which is always a bit inaccurate. The values have been computed by picking a random point from the model itself (the curve, so a real random point). Seven other values are picked, with a mutual distance of 45° , in order to get eight samples corresponding with the eight antennas. These samples form the measurement that is converted to obtain the angle. This is performed 100 times, each result is compared with the real angle and the average error is obtained. This error can be reduced by improving the resolution: using more reference points. If the conversion would be perfect, this error should be 0° .

The antennas mutual deviation differs depending on the ϕ -angle, and is shown before in the error bars from figure 7.15 (p. 17) This deviation depends on the manufacturing precision of the antennas and can only be reduced by calibrating each individual antenna thoroughly.

To obtain the values, again 100 random measurements were obtained like in the previous test. The only difference now is that each antenna included a small shift. This shift came from a normally distributed random value, with the standard deviation that fits the model at that specific ϕ -angle. An illustration on how this measurement is created, is shown in figure 7.23.

This test results in an error where the error from the

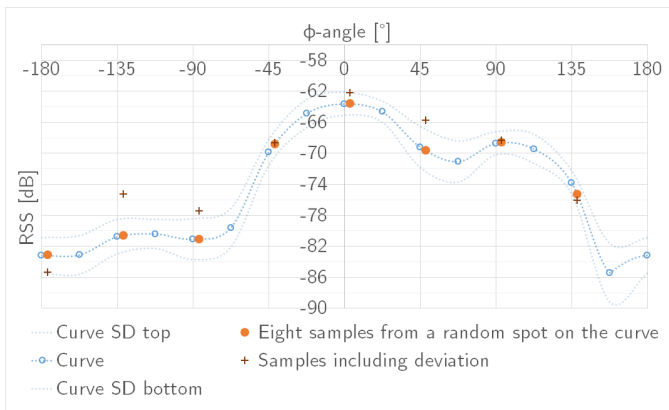


Figure 7.23: Virtual environment to create a test measurement from a model.

Table 7.3: Decrease of error by internal deviation, by increasing number of samples.

$\theta = 0^\circ$	Average ϕ -error					
	n=1	n=2	n=3	n=4	n=6	n=8
	$\pm 3.34^\circ$	$\pm 2.18^\circ$	$\pm 1.89^\circ$	$\pm 1.88^\circ$	$\pm 1.38^\circ$	$\pm 1.26^\circ$

converter is also present. To distinguish between these errors, the error from the converter is subtracted using the Pythagorean theorem: $\sigma_{antenna}^2 = \sigma_{total}^2 - \sigma_{converter}^2$ (where σ can be both the average deviation or the standard deviation). If the errors are combined, it will result in ($\sqrt{1.33^2 + 1.35^2} =$) 1.89 for $\theta = 45^\circ$, 1.70 for $\theta = 0^\circ$ and 1.61 for $\theta = -45^\circ$. These values can be compared to the ones in figure 7.22 and table 7.1. The difference with that test is that it was based on ten measurements between $\phi = 0^\circ$ and $\phi = 45^\circ$, while this test is based on automatically generated measurements of random points.

The antennas internal deviation is the inaccuracy of the measurement to determine the RSSI from one sample. It differs depending on the ϕ -angle, and is shown before in the error bars from figure 7.13 (p. 15). According to the Central Limit Theorem, this deviation can be reduced by taking the average of multiple measurements – consuming more time and power.

The same test as from the mutual deviation is performed, now with the internal standard deviation which is bigger. 100 test measurements are converted into an estimated AOA, the deviation of this angle compared to the true angle is collected and the converter error is subtracted.

As mentioned, the internal error can be reduced by collecting multiple samples and using the average of those. This is demonstrated in table 7.3, for $\theta = 0^\circ$ only (and including AGO). For every value of n , a sample with a random internal deviation is created n times for every antenna, from which the average is used to estimate the AOA 100 times.

In theory, the error can be treated as the standard deviation of a probability experiment. The Pythagorean theorem can be used to calculate the sum of n standard deviations from normally distributed random variables: $\sigma_{sum}^2 = \sigma_1^2 + \sigma_2^2 + \dots + \sigma_n^2$. Computing the *average* of n standard deviations, like performed in this test, requires one more step: dividing this

Table 7.4: Deviation caused by target orientation.

	Average ϕ -error		
	Dongle backside	Dongle backside upside down	Dongle upside down
$\theta = 45^\circ$	$-12.91 \pm 8.04^\circ$	$-4.67 \pm 8.16^\circ$	$-5.41 \pm 10.24^\circ$
$\theta = 0^\circ$	$3.78 \pm 4.78^\circ$	$21.99 \pm 8.15^\circ$	$16.92 \pm 4.91^\circ$
$\theta = -45^\circ$	*	*	$15.43 \pm 7.40^{\circ**}$

*rate was too high
**rate was too high, model $\theta = 0^\circ$ was used

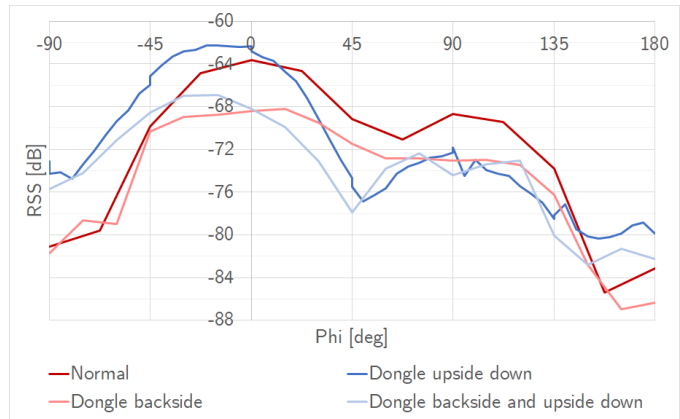


Figure 7.24: Influence of the dongle orientation on the test results

sum by n . After rewriting, the formula becomes as follows where \bar{x} stands for the average error in degrees:

$$\bar{x} = x_{n=1} * \frac{1}{\sqrt{n}}$$

This equation approaches the values from table 7.3 quite accurate, using $x_{n=1} = \pm 3.34$. It can be used to predict the error from any other model and any amount of samples.

The target orientation or polarization. So far, the inaccuracies from the converter and the antennas were all based on tests where the target faced the PCB with one side (in this case: the topside of the USB-dongle). It appeared that the reception changed drastically when the target was oriented differently, as shown in figure 7.24. The influence of this on the localization error is shown in table 7.4.

For $\theta = 0^\circ$, the change of the model is quite predictable. Combining the error from using the backside of the dongle with the error from having the dongle upside down, creates a new error that is surprisingly close to the measured error:

$$3.78 + 4.91 = 20.7 \approx 21.99$$

$$\pm (\sqrt{4.78^2 + 4.91^2} = 6.85 \approx 8.15).$$

However, the shape of the model has changed and even more so for the other two tilts. For $\theta = -45^\circ$, the shape was even so badly changed that the rates became too high: other models had a lower rate but a worse estimation. Only for the measurement with the dongle upside down, the model from $\theta = 0^\circ$ could give a somewhat reliable estimation.

These experiments show that the polarization of the signal (based on the orientation of the target compared to the PCB) has a huge influence on the accuracy. There are two ways to deal with this problem. One is to create new models based

on different orientations of the target. Besides ϕ -angle and θ -angle, also the polarization can now be derived. Because the shape of the models at $\theta = 0^\circ$ are so much alike, these will easily be confused and an error seems inevitable. Furthermore, other circumstances like reflections of the signal caused by surrounding objects would also heavily change the shape of the reception. In the end, it would be unlikely that the PCB can distinct all the different shapes. The second solution would be to use an isotropically radiating antenna as the target, or an omnidirectional radiating antenna where the up- and downside are fixed. This might decrease the change in polarization as much as possible.

The effect is also visible at $\theta = 90^\circ$ and $\theta = -90^\circ$. One would expect that the ϕ -angle does not make a difference any more when the target is located perpendicular to the PCB, but in fact it does. Rotating the ϕ -angle at this setup is equal to rotating the dongle upside down, and the top and bottom of the antennas are susceptible to this effect. One test (not displayed) showed variations up to 10 dB. One antenna even got two results at the same angle, at different measurements, that were 9 dB apart. This angle seems very unreliable and is not further investigated.

Concluding this section, some sources of inaccuracy have been investigated: the internal and mutual deviations from the antennas and the converter error. From the error caused by the polarization, only a grasp has been captured.

There are still a lot of uncertainties that have not been investigated. One is the earlier mentioned change of signal reception caused by reflections of surrounding objects. Both small scale and large scale fading will have their influence within the warehouse's indoor environment. What has not been mentioned yet, is the change of the errors based on time and environmental temperature. All the experiments that have provided the data of this research, were performed within hours in an anechoic chamber with a controlled temperature. The errors might easily change a bit over time, or be influenced by temperature change. They are actually no more than an indication on how the PCB would perform in reality.

I. Number of antennas

This PCB has eight antennas but in theory six, four or even three antennas could be sufficient to derive the AOA. The downside is that the accuracy will probably decrease: there are less points to compare with the model, each deviation has a bigger influence and chances are that the measurement fits multiple places on the model. The use of more antennas should make the predictions more accurate.

Several simulations with the same system with only four antennas have been performed to show this, as well as with 16 antennas to show the opposite effect. Like in the previous section, 100 random measurements have been created but now for four and sixteen antennas. The results are shown in table 7.5, together with the performance of eight antennas from table 7.2 (p. 20). It appears clearly that a bigger number of antennas results in a smaller error. The only exception of this is the converter error at $\theta = -45^\circ$. There is no clear explanation for this.

Table 7.5: Accuracy difference based on number of antennas.

Source of inaccuracy	Average ϕ -error			
	4 ant.	8 ant.	16 ant.	
Converter:	$\theta = 45^\circ$	$\pm 0.88^\circ$	$\pm 1.33^\circ$	$\pm 0.27^\circ$
	$\theta = 0^\circ$	$\pm 1.82^\circ$	$\pm 0.37^\circ$	$\pm 0.32^\circ$
	$\theta = -45^\circ$	$\pm 0.76^\circ$	$\pm 0.48^\circ$	$\pm 0.41^\circ$
Antenna (mutual):	$\theta = 45^\circ$	$\pm 5.80^\circ$	$\pm 1.35^\circ$	$\pm 0.90^\circ$
	$\theta = 0^\circ$	$\pm 10.65^\circ$	$\pm 1.66^\circ$	$\pm 1.03^\circ$
	$\theta = -45^\circ$	$\pm 4.48^\circ$	$\pm 1.54^\circ$	$\pm 0.99^\circ$



Figure 7.25: Test setup bicycle cellar

There are some new problems when only four antennas are used. Model $\theta = 0^\circ$ has a point where the four measurement samples fit the model twice: once at the right ϕ -angle and once 56° shifted to the other side of the lobe. Two of the hundred tests had an error of this size. They are considered outliers and ignored for the computation of the converter error. This feature however happens more often when the mutual deviation is added to the samples. Many times the converter estimates the AOA more than 30° shifted to the right or left from the real ϕ -angle. One estimation was even at -176° : almost perfectly in the opposite direction. A good reason that model $\theta = 0^\circ$ has a bigger problem with the changed layout, is that there is more symmetry in it: the two lobes are at 90° distance and have the same shape left and right, easily to be confused with each other.

Knowing this, it is strongly advised to use more than four antennas.

J. Indoor experiment

A final test is performed indoor, where the reception will severely be influenced by NLOS and reflections. The test setup is displayed in figure 7.25. The PCB and dongle are put 125 cm above the ground using tripods. They are placed in a bicycle cellar of 17.00m x 6.15m, with pillars as drawn in figure 7.26. The PCB is also drawn in this figure, and the placements of the dongle are illustrated as blue dots. For every measurement, a ϕ -angle is estimated based on model $\theta = 0^\circ$ from the anechoic chamber. The displacement of this angle compared to the true angle is drawn in red on figure 7.26 for each dongle location.

The figure shows quite diverse results. The model is clearly not representative any more when compared to the indoor reception. Especially the measurements with NLOS and located

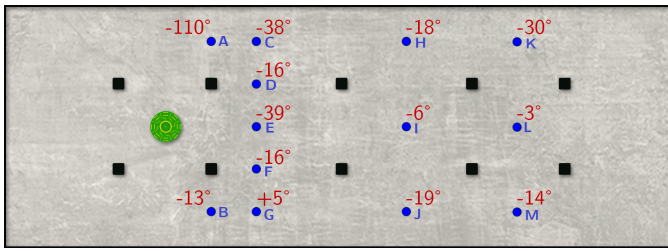


Figure 7.26: Indoor test measurements and corresponding errors

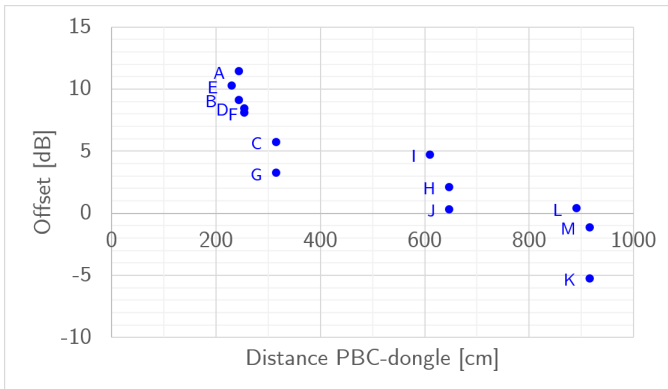


Figure 7.27: Signal strength against distance

the furthest away, had a more evenly distributed RSS on every antenna. In many cases the side lobe was less present on the measurements, resulting in a shift of the estimated ϕ -angle to the left (hence all the minus signs in figure 7.26).

Also the distance to the target can be calculated based on the Automatically Generated Offset (AGO), as mentioned in the end of section VII-F. In theory, an offset of 0 means that the signal was as strong as from 240 cm in the anechoic chamber. In the cellar, the signal reflects on the walls and produces a stronger measurement than in the anechoic chamber. The five closest measurements (between 230 and 250 cm) therefore gained an offset between 8 and 11.5 (comparable to the difference between 8dB and 11.5 dB). Furthermore, the offset depends also on the estimated AOA so an inaccurate estimated ϕ -angle would lead to an inaccurate proximity estimation. Figure 7.27 shows a plot of the offset of each measurement spot, against the distance between the spot and the PCB. It shows a logarithmic decay and suggests a Path Loss Exponent (see section VII-E, p. 18) between 1.5 and 2.0. The spots with a pillar blocking the direct LOS – being C, G, K and M – seem to have a lower signal strength. The measurements are yet so diverse that the distance can be approximated with an accuracy of around 50%: measurement G would for example be approximated at 500 cm distance and I at 400 cm.

K. Conclusions

The PCB functions as a switched-beam antenna system and is able to trace the AOA of a Bluetooth signal. To achieve this, the reception of a signal from different angles needs to be modelled in advance. Measurements have shown that there is not one model to determine the AOA. Depending on the tilt (or

θ -angle), the distribution of reception over the eight antennas changes its shape significantly. Based on this shape, not only the ϕ -angle but also the θ -angle need to be determined.

A method to determine the AOA using three models has shown to reach an accuracy of around 2° , but only in the horizontal plane close to the altitude of where the three models were formed and without reflections from the environment. Increasing the number of models would increase the accuracy and coverage. Using the system in an indoor environment requires again a new model. The effect of NLOS and reflecting walls has a big influence on the performance inside a warehouse. The accuracy also increases with the number of directional antennas that are being used to trace the AOA, though the use of eight antennas (like in this particular PCB) should be sufficient. The improvement of accuracy when the number of antennas is doubled, is not so significant: reflections and absorption will form a much higher source of distortion.

The distance to the target can be derived from the Automatically Generated Offset (AGO) if the Path Loss Exponent (PLE) is known and the estimated AOA is accurate enough. Until now, the accuracy is approximately 50%.

The orientation of the target has a big influence on the reception within this testing environment. The current models were not functioning properly any more when the target was put upside down or backwards. In the same perspective, the behaviour at $\theta = -90^\circ$ and $\theta = 90^\circ$ is unclear.

Even with an accuracy of less than 40° , the estimation of AOA can be of added value in positioning a target. This PCB can play a part in realizing the pallet monitoring inside a warehouse. Still, there is a lot left to investigate before this end goal is achieved.

VIII. FUTURE STUDY

Now so much about the behaviour of the PCB is cleared up, the next step is to improve the system for indoor usage. After that, the localization architecture is yet unclear: how can the PCBs be installed to reach a high efficiency? What trade off in metrics defines this efficiency? How can the implementation of smart forklifts contribute to a better system? Furthermore, the part about accurate positioning has not been treated yet. This section will give an overview of possible future study on this subject. Also, some hypothesis are given.

A. Improvements

When the same tests are performed at an indoor environment with reflecting walls and objects blocking the line of sight, new models can be formed. One can also take the models from an anechoic chamber, include the effects of polarization and regard the indoor environment as the sum of these signals coming from all directions. This way, it might be possible to translate a measurement into the **AOA of a signal and multipath components**. An elaborate estimation method or multiple signal classifier is required to achieve this. Because there are so many factors like the polarization, θ -angle change of pattern and self-interference by multipath components, this will probably be a very big challenge.

At least, the converter used in this research (converting a measurement into an estimated AOA based on models and the rate of deviation) seems too inefficient and there must be possible methods that perform better.

The effects of **change over time, humidity and temperature influence** is also not taken into account. Future study must show how much this affects the PCB behaviour.

When a measurement is compared to the model, often more than one comparison has a local low rate of diversion. The current system picks the lowest one but in practice, the history of the object its location can be used to pick the lowest rate close to the old angle of arrival. The **history** or **mobility** of a target can be used to improve the positioning.

B. Architecture

The accuracy of the system has yet only been described in terms of deriving the AOA. The accuracy of the end product must be translated into positioning a target in a plain or 3-D area including the certainty. It would be useful to investigate how this accuracy is influenced by metrics like the **height** of the ceiling, the **presence of obstacles** and the **placement (pattern, grid, density) of the PCBs**.

There will be a trade-off between the number of gateways required and the gain of accuracy of the fast positioning. If the density increases and the gain becomes small or the required accuracy is reached, an optimum is found. Of course, this depends on the height of the ceiling and the presence of obstructions.

Considering the height of the ceiling, it makes sense that the accuracy of the positioning decays with the distance – between measurement device and mobile target – squared. The RSS value of a gateway nearby is more accurate than that of a gateway further away. At least three references are required to estimate a position and the reliability can be weighted with the distance to the target. The accuracy of the estimation of the AOA is comparable, but it is also expected that there will be more multipath interference when reflecting objects are near the measuring device. A proper **distance to the ceiling and to the top of the racks** for the PCB must in this case be found.

Because it is also possible to perform positioning using RSS only, the **added value of angulation** in this system can be evaluated. There will probably be a trade off between increasing the density of gateways and adding the angulation method to gain a similar positioning accuracy.

The **addition of smart forklifts** brings a whole new set of topics like how they measure altitude and which of the suggested options (see section V-A, p. 11) is most optimal to implement.

C. Accurate positioning

Looking back to section V, the research in this paper was only about the fast positioning method. The proposed accurate positioning method used static beacons located around the

RTIs. Future study must show how (which pattern, grid, density) these **beacons can best be placed**, how this placement changes for a **2-D instead of a 3-D** positioning system and what the impact is of the **presence of obstacles**.

Also, an optimum must be found in the **advertisement frequency and transmit power** of the beacons to keep the power consumption of the mobile target low, the power consumption of the beacons reasonable and not overwhelm the ether but still be able to perform sufficient accurate positioning.

REFERENCES

- [1] Neal Patwari, Joshua N Ash, Spyros Kyperountas, Alfred O Hero, Randolph L Moses, and Neiyer S Correal. Locating the nodes: cooperative localization in wireless sensor networks. *IEEE Signal processing magazine*, 22(4):54–69, 2005.
- [2] Jean Kumagai and Steven Cherry. Sensors and sensibility. *IEEE Spectrum*, 41(7):22–26, 2004.
- [3] L. Evers, M.J.J. Bijl, M.J.J. Bijl, Mihai Marin Perianu, Raluca Marin Perianu, and Paul J.M. Havinga. *Wireless Sensor Networks and Beyond: A Case Study on Transport and Logistics*. Centre for Telematics and Information Technology (CTIT), 2005.
- [4] Leon Evers, Paul JM Havinga, Jan Kuper, MEM Lijding, and Nirvana Meratnia. Sensorscheme: Supply chain management automation using wireless sensor networks. In *Emerging Technologies and Factory Automation, 2007. ETFA. IEEE Conference on*, pages 448–455. IEEE, 2007.
- [5] Menasheh Fogel, Nathan Burkhart, Hongliang Ren, Jeremy Schiff, Max Meng, and Ken Goldberg. Automated tracking of pallets in warehouses: Beacon layout and asymmetric ultrasound observation models. In *Automation Science and Engineering, 2007. CASE 2007. IEEE International Conference on*, pages 678–685. IEEE, 2007.
- [6] Sarah Spieker and Christof Rohrig. Localization of pallets in warehouses using wireless sensor networks. In *Control and Automation, 2008 16th Mediterranean Conference on*, pages 1833–1838. IEEE, 2008.
- [7] Dennis JA Bijwaard, Wouter AP van Kleunen, Paul JM Havinga, Leon Kleiboer, and Mark JJ Bijl. Industry: Using dynamic wsns in smart logistics for fruits and pharmacy. In *Proceedings of the 9th ACM Conference on Embedded Networked Sensor Systems*, pages 218–231. ACM, 2011.
- [8] Encyclopedia of Small Business. Logistics and Transportation - levels, system, manager, definition, type, business, system. <http://www.referenceforbusiness.com/management/Log-Mar/Logistics-and-Transportation.html>. Accessed: 2017-12-19.
- [9] Transport Equipment — GLN Allocation Rules — GS1. <https://www.gs1.org/1/tlkeys/index.php?p=asset/aid=39>. Accessed: 2017-12-19.
- [10] Zahid Farid, Rosdiadee Nordin, and Mahamod Ismail. Recent Advances in Wireless Indoor Localization Techniques and System. *Journal of Computer Networks and Communications*, 2013:1–12, sep 2013.
- [11] Hui Liu, Houshang Darabi, Pat Banerjee, and Jing Liu. Survey of Wireless Indoor Positioning Techniques and Systems. *IEEE Transactions on Systems, Man and Cybernetics, Part C (Applications and Reviews)*, 37(6):1067–1080, nov 2007.
- [12] J. Hightower and G. Borriello. Location systems for ubiquitous computing. *Computer*, 34(8):57–66, 2001.
- [13] Mai A Al-Ammar, Suheer Alhadhrami, Abdulmalik Al-Salman, Abdulrahman Alarifi, Hend S Al-Khalifa, Ahmad Alnafessah, and Mansour Alsaleh. Comparative survey of indoor positioning technologies, techniques, and algorithms. In *Cyberworlds (CW), 2014 International Conference on*, pages 245–252. IEEE, 2014.
- [14] Yanying Gu, Anthony Lo, and Ignas Niemegeers. A survey of indoor positioning systems for wireless personal networks. *IEEE Communications surveys & tutorials*, 11(1):13–32, 2009.
- [15] Zain Bin Tariq. 57 Non-GPS Positioning Systems: A Survey. *ACM Comput. Surv. Article*, 50(34), 2017.
- [16] Yapeng Wang, Xu Yang, Yutian Zhao, Yue Liu, and Laurie Cuthbert. Bluetooth positioning using rssi and triangulation methods. In *Consumer Communications and Networking Conference (CCNC), 2013 IEEE*, pages 837–842. IEEE, 2013.
- [17] Xin Hu, Lianglun Cheng, and Guangchi Zhang. A zigbee-based localization algorithm for indoor environments. In *Computer Science and Network Technology (ICCSNT), 2011 International Conference on*, volume 3, pages 1776–1781. IEEE, 2011.
- [18] Sinan Gezici. A survey on wireless position estimation. *Wireless personal communications*, 44(3):263–282, 2008.
- [19] Nissanka B Priyantha, Anit Chakraborty, and Hari Balakrishnan. The cricket location-support system. In *Proceedings of the 6th annual international conference on Mobile computing and networking*, pages 32–43. ACM, 2000.
- [20] Myungkyun Kwak and Jongwha Chong. A new double two-way ranging algorithm for ranging system. In *Network Infrastructure and Digital Content, 2010 2nd IEEE International Conference on*, pages 470–473. IEEE, 2010.
- [21] Christian Gentner and Thomas Jost. Indoor positioning using time difference of arrival between multipath components. In *Indoor Positioning and Indoor Navigation (IPIN), 2013 International Conference on*, pages 1–10. IEEE, 2013.
- [22] Samuel House, Sean Connell, Ian Milligan, Daniel Austin, Tamara L Hayes, and Patrick Chiang. Indoor localization using pedestrian dead reckoning updated with rfid-based fiducials. In *Engineering in Medicine and Biology Society, EMBC, 2011 Annual International Conference of the IEEE*, pages 7598–7601. IEEE, 2011.
- [23] Deepak Pai, Inguva Sasi, Phani Shekhar Mantripragada, Mudit Malpani, and Nitin Aggarwal. Padati: A robust pedestrian dead reckoning system on smartphones. In *Trust, Security and Privacy in Computing and Communications (TrustCom), 2012 IEEE 11th International Conference on*, pages 2000–2007. IEEE, 2012.
- [24] Ming Ren and Hassan A Karimi. Movement pattern recognition assisted map matching for pedestrian/wheelchair navigation. *The journal of navigation*, 65(4):617–633, 2012.
- [25] Mohammed A Quddus, Washington Y Ochieng, and Robert B Noland. Integrity of map-matching algorithms. *Transportation Research Part C: Emerging Technologies*, 14(4):283–302, 2006.
- [26] Shaowei Yang and Bo Wang. Residual based weighted

- least square algorithm for bluetooth/UWB indoor localization system. In *2017 36th Chinese Control Conference (CCC)*, pages 5959–5963. IEEE, jul 2017.
- [27] Yu Gu, Lianghu Quan, Fuji Ren, and Jie Li. Fast Indoor Localization of Smart Hand-Held Devices Using Bluetooth. In *2014 10th International Conference on Mobile Ad-hoc and Sensor Networks*, pages 186–194. IEEE, dec 2014.
- [28] Zhu Jianyong, Luo Haiyong, Chen Zili, and Li Zhaohui. Rssi based bluetooth low energy indoor positioning. In *Indoor Positioning and Indoor Navigation (IPIN), 2014 International Conference on*, pages 526–533. IEEE, 2014.
- [29] Deliang Liu, Kaihua Liu, Yongtao Ma, and Jiexiao Yu. Joint toa and doa localization in indoor environment using virtual stations. *IEEE Communications Letters*, 18(8):1423–1426, 2014.
- [30] Ilan Ziskind and Mati Wax. Maximum likelihood localization of multiple sources by alternating projection. *IEEE Transactions on Acoustics, Speech, and Signal Processing*, 36(10):1553–1560, 1988.
- [31] Richard Roy and Thomas Kailath. Esprit-estimation of signal parameters via rotational invariance techniques. *IEEE Transactions on acoustics, speech, and signal processing*, 37(7):984–995, 1989.
- [32] Ralph Schmidt. Multiple emitter location and signal parameter estimation. *IEEE transactions on antennas and propagation*, 34(3):276–280, 1986.
- [33] Zhilong Shan and T-SP Yum. A conjugate augmented approach to direction-of-arrival estimation. *IEEE Transactions on Signal Processing*, 53(11):4104–4109, 2005.
- [34] Anthony J Devaney. Time reversal imaging of obscured targets from multistatic data. *IEEE Transactions on Antennas and Propagation*, 53(5):1600–1610, 2005.
- [35] Weile Zhang, Qinye Yin, Hongyang Chen, Feifei Gao, and Nirwan Ansari. Distributed angle estimation for localization in wireless sensor networks. *IEEE Transactions on Wireless communications*, 12(2):527–537, 2013.
- [36] Zhilong Shan and Tak-Shing P Yum. Precise localization with smart antennas in ad-hoc networks. In *Global Telecommunications Conference, 2007. GLOBECOM'07. IEEE*, pages 1053–1057. IEEE, 2007.
- [37] Gianni Giorgetti, Alessandro Cidronali, Sandeep KS Gupta, and Gianfranco Manes. Single-anchor indoor localization using a switched-beam antenna. *IEEE Communications Letters*, 13(1):58–60, 2009.
- [38] P Kulakowski. Beacons with rotating beams in aoa localization technique for wsn. *COST 2100 TD (08)*, 544, 2008.
- [39] Bobin Yao, Wenjie Wang, Wei Han, and Qinye Yin. Distributed angle estimation by multiple frequencies synthetic array in wireless sensor localization system. *IEEE Transactions on Wireless Communications*, 13(2):876–887, 2014.
- [40] Sheng Zhou and John K Pollard. Position measurement using bluetooth. *IEEE Transactions on Consumer Electronics*, 52(2):555–558, 2006.
- [41] Guoqiang Mao, Brian DO Anderson, and Barış Fidan.

Path loss exponent estimation for wireless sensor network localization. *Computer Networks*, 51(10):2467–2483, 2007.

ATTRIBUTIONS

Icons from figure 2.1 on page 2 made by Vectors Market from www.flaticon.com.

Figure 3.3 on page 5 from [16]. The icons from this figure are also used in figure 3.4, 3.5, 4.6, 4.7, 4.8 and 5.9 which are made by the author.

Figure 6.10 is made by the author, but a model from the PCB is used that was made by D.T.N. Nguyen – the inventor of the PCB. Figure 7.11, 7.12, 7.22, 7.25 and 7.26 are made by the author. Figure 7.13, 7.15, 7.19, 7.20, 7.23, 7.24, 7.27 and the small one in section VII-D are made by the author using Microsoft Excel. Figure 7.14, 7.16, 7.17, 7.18 and 7.21 are made by author using Matlab.

The anechoic chamber was provided by the Telecommunication Engineering group from the University of Twente. It was build according to the design of a “3 m semi anechoic chamber”.

Some features of the chamber:

- Full compliance emission test site for frequency range of 30MHz to 18GHz as per CISPR 16-1-4
- Full compliance immunity test site for frequency range of 80MHz to 6GHz as per IEC/EN 61000-4-3
- Shielding effectiveness according to EN 50147-1 (>80dB at 10kHz)

The chamber was caged in 2mm ZMA-140 galvanized shielding panels, provided with a hybrid solution of ferrite tiles and polystyrene hybrid absorbers (model HT45) on walls, ceiling and floor.

The Bluetooth Smart USB dongle was a Bluegiga BLE112, controlled with a Python script.